Higher-dimensional operators at finite temperature affect gravitational-wave predictions

Bernardo, Fabio; Klose, Philipp; Schicho, Philipp; Tenkanen, Tuomas V.I.

How to cite

BERNARDO, Fabio et al. Higher-dimensional operators at finite temperature affect gravitational-wave predictions. In: The journal of high energy physics, 2025, vol. 08, n° 8, p. 109. doi: 10.1007/JHEP08(2025)109

This publication URL: https://archive-ouverte.unige.ch/unige:190875
Publication DOI: 10.1007/JHEP08(2025)109

Published for SISSA by Springer

Received: April 11, 2025
Revised: June 20, 2025
Accepted: July 14, 2025
Published: August 14, 2025

Higher-dimensional operators at finite temperature affect gravitational-wave predictions

Fabio Bernardo,[a] **Philipp Klose**,[b,c,d] **Philipp Schicho**[a] **and Tuomas V.I. Tenkanen**[e]

[a] *Département de Physique Théorique, Université de Genève, 24 quai Ernest Ansermet, CH-1211 Genève 4, Switzerland*
[b] *AEC, Institute for Theoretical Physics, University of Bern, Sidlerstrasse 5, CH-3012 Bern, Switzerland*
[c] *Fakultät für Physik, Bielefeld University, Universitätsstrasse 4, 33615 Bielefeld, Germany*
[d] *Theory group, Dutch National Institute for Subatomic Physics (Nikhef), Science Park 105, 1098 XG Amsterdam, Netherlands*
[e] *Department of Physics and Helsinki Institute of Physics, P.O. Box 64, FI-00014 University of Helsinki, Finland*

E-mail: fabio.bernardo@unige.ch, pklose@nikhef.nl, philipp.schicho@unige.ch, tuomas.tenkanen@helsinki.fi

Abstract: We investigate the effect of higher-dimensional marginal operators on the thermodynamics of cosmological phase transitions. Using the Abelian Higgs model as a representative for radiatively-generated one-step transitions, we systematically match these operators, which arise at higher orders in the underlying high-temperature expansion of thermal effective field theory, and use field redefinitions to construct a complete, minimal, and gauge-invariant operator basis. The Abelian Higgs model shares the essential infrared structure of more realistic gauge-Higgs theories at high temperatures, allowing us to test the validity of dimensional reduction in a simplified setting. We argue that for strong transitions, temporal gauge modes, which enhance the transition strength, should be treated on equal footing with spatial ones. Marginal operators are found to weaken the transition and introduce significant uncertainties for strong transitions. For transitions strong enough to produce gravitational waves detectable by LISA, our findings suggest that the high-temperature expansion may break down entirely. This would limit the applicability of effective theory techniques, including their use in non-perturbative lattice studies.

Keywords: Cosmology of Theories BSM, Effective Field Theories, Phase Transitions in the Early Universe, Thermal Field Theory

ArXiv ePrint: 2503.18904

https://doi.org/10.1007/JHEP08(2025)109

Contents

1 Introduction

Cosmological phase transitions offer a compelling window into the physics of the early universe, potentially resulting in observational signatures such as gravitational waves (GWs). Since the Standard Model does not exhibit a thermal phase transition [1–5], GWs from strong first-order phase transitions would provide a particularly promising probe for new physics beyond the Standard Model (BSM) [6]. Effective field theory (EFT) techniques such as dimensional reduction at high temperatures [7, 8] play a central role in describing these transitions. However, the effect of higher-dimensional marginal operators that arise from higher-order matching contributions in the underlying high-temperature expansion, and especially their impact on non-perturbative phenomena, remains an open question.

In the context of electroweak theories, this issue was framed more precisely in the seminal reference [7], which stated that, apart from simple power-counting estimates, it remains

JHEP08(2025)109

difficult to comprehensively assess the importance of dimension-six operators. While there are comprehensive studies that have since examined the impact of parity-violating marginal operators in the electroweak sector of the SM [9], fermion-induced operators in the minimal SM [10], and marginal operators in effective theories of hot QCD [11–13], analogous estimates for gauge-Higgs theories beyond the SM have indeed remained a long-standing challenge. However, several recent works have reported simple estimates of the impact of higher-dimensional operators in thermal EFTs for the Two-Higgs Doublet model [14–16], singlet [17–20] and triplet [21] extensions of the SM, SMEFT [22, 23], and other theories [24–26].

The primary goal of this work is to extend these investigations by providing a comprehensive study on the impact of higher-dimensional operators in the Abelian Higgs model. This simplified toy setup captures many key features of more complex gauge-Higgs theories and BSM scenarios, including the role of temporal gauge fields, the hierarchy between gauge and scalar modes, and radiative barrier formation, which result in a qualitatively similar infrared structure at high temperatures. These structural similarities make the Abelian Higgs model a useful proxy for studying cosmological phase transitions in generic gauge-Higgs theories. However, applications to more intricate BSM theories are beyond the scope of this article and are left for future work.

Notably, [24] found that even in the SM, the matching contribution to the Wilson coefficient of the sextic $(\phi^\dagger\phi)^3$ operator is gauge-dependent. This indicates that the chosen operator basis for the matching is incomplete. Similar gauge-dependence issues, related to the singlet-Higgs portal, have been reported in the singlet-extended SM [27]. Using the Abelian Higgs model as a case study, we explicitly demonstrate how to overcome such problems by employing field redefinitions to construct a minimal and fully gauge-invariant operator basis. This approach not only ensures the theoretical consistency of thermal EFTs but also clarifies the limitations of perturbative expansions in describing strong phase transitions. We emphasize that an incomplete operator basis can introduce gauge artifacts, leading to ambiguities in the computation of condensates and other thermodynamic quantities. These deficiencies may, in turn, propagate into uncertainties in predictions of the GW spectrum and other observables derived from the EFT.

Our findings directly impact the interpretation of potential future GW signals and aid in assessing the reliability of non-perturbative studies in regimes where marginal operators may not be negligible. Importantly, [17] demonstrated that any model which maps onto a SM-like effective theory without marginal operators in the infrared (IR) cannot produce phase transitions strong enough to be detectable by LISA. This result clearly motivates the inclusion of marginal operators in effective theories to accurately describe the strongest transitions. Recently, it was also demonstrated how higher-dimensional operators can influence the GW spectrum in the Yukawa model [28] and the electroweak sector of the SM EFT [29] further underscoring the importance of systematically incorporating them into EFT descriptions. In particular, they can alter the transition dynamics and, consequently, the properties of the predicted GWs. In fact, [28, 29] found that phase transitions strong enough to be observable in LISA-generation GW detectors, often occur near the boundary of EFT validity. In this work, we conduct a similar analysis and arrive at comparable conclusions. Our results demonstrate that neglecting marginal operators can introduce uncertainties of up to $\mathcal{O}(5\%)$

JHEP08(2025)109

even for moderately strong transitions. These uncertainties can be significant compared to those from other sources in perturbative approaches and non-perturbative lattice simulations. For the strongest transitions, which are characterized by large discontinuities in the scalar background field and the resulting large Higgs mechanism-induced mass contributions, our results suggest a breakdown of the high-temperature expansion. This breakdown would severely limit the reliability of perturbative and non-perturbative methods that rely on such an expansion. In this context, our results build on and strengthen the conclusions of [17], suggesting that one-step phase transitions with radiatively generated barriers, strong enough to be detectable by LISA, may face a serious breakdown of the high-temperature expansion. This breakdown would imply that new methods beyond the standard effective dimensional reduction framework at high temperature need to be devised. While our analysis is performed in a simplified toy model, its key features, such as the IR behavior and the structure of the dimensional reduction mapping, especially the generation of marginal operators, are shared by more realistic gauge-Higgs theories, including the SU(2) gauge-Higgs model studied in [17].

It remains unclear how to include marginal operators in state-of-the-art, lattice simulations of high-temperature EFTs. While they may be necessary to describe very strong first-order transitions, they break the super-renormalizability of such theories and compromise the exact lattice-continuum relations required to interpret lattice simulation results [30–32]. In practice, direct lattice simulations of full theories are not feasible if they contain fermions with non-Abelian chiral gauge couplings [33], though some approaches treat the fermionic sector perturbatively [4, 34, 35]. This highlights the need to develop techniques to compute phase transition thermodynamics entirely without relying on high-temperature expansions — an endeavor we leave for future work. As shown in [20], this is especially relevant for BSM theories with heavy additional scalars and large portal couplings to the Higgs.

The structure of this paper is as follows. Section 2 introduces the Abelian Higgs model, followed by its dimensional reduction to thermal effective field theories in section 3, with a focus on the role of dimension-six operators and the temporal gauge mode. In section 4, we compute thermodynamic properties and discuss constraints on the validity of the effective theory, emphasizing the role of higher-dimensional operators in modifying the transition strength. In section 5, we briefly discuss the computation of three thermal parameters required for predicting a GW background using results of hydrodynamic simulations [36]. Finally, section 6 summarizes our findings and outlines future directions. The main text is supplemented by detailed appendices. Appendix A provides an overview of relevant field redefinitions. The renormalization, β-functions, and operator matching for integrating out the hard scale are covered in appendix B and for integrating out the soft scale in appendix C.

2 Model

We consider the Abelian Higgs model[1] at finite temperature [37–39]. The corresponding four-dimensional (4d) Euclidean Lagrangian density is

$$\mathcal{L}^{\mathrm{4d}} = \frac{1}{4}F_{\mu\nu}F_{\mu\nu} + (D_\mu\phi_4)^\dagger(D_\mu\phi_4) + \mu^2\phi_4^\dagger\phi_4 + \lambda(\phi_4^\dagger\phi_4)^2 \,, \tag{2.1}$$

[1] Also known as Scalar electrodynamics, Scalar QED or U(1)-Higgs theory.

JHEP08(2025)109

where B_μ is a U(1) gauge field with gauge coupling g and ϕ_4 a complex scalar field. The covariant derivative of the complex Higgs field reads $D_\mu\phi_4 = \partial_\mu\phi_4 - igY_\phi B_\mu\phi_4$, the field strength tensor $F_{\mu\nu} = \partial_\mu B_\nu - \partial_\nu B_\mu$, and the hypercharge for the complex scalar $Y_\phi = 1$. Since our goal is to compute the equilibrium thermodynamics (as well as the statistical part of the bubble nucleation rate) of this model, we already define the Lagrangian in a Euclidean (rather than Minkowski) spacetime. One can express the complex field in terms of real fields,

$$\phi_4 = \frac{1}{\sqrt{2}}\left(v_4 + h_4 + i\chi_4\right) \,, \tag{2.2}$$

where v_4 is a scalar background field and h_4 and χ_4 are propagating mass eigenstates. We apply general R_ξ (or Fermi) gauge fixing [40, 41],

$$\mathcal{L}_{\rm GF}^{R_\xi} = \frac{1}{2\xi}\left[F(\phi_4, \phi_4^\dagger)\right]^2 \,, \quad F(\phi_4, \phi_4^\dagger) \equiv -\partial_\mu B_\mu \,, \tag{2.3}$$

with the gauge fixing functional $F(\phi_4, \phi_4^\dagger)$. This implies the corresponding ghost Lagrangian

$$\mathcal{L}_{\rm FP} = \bar{c}(-\Box)c \,, \tag{2.4}$$

where $c, (\bar{c})$ are (anti)ghost fields. Gauge-fixing choices are comprehensively discussed in [40, 41]. In this simple model, the ghosts completely decouple from other sectors and do not affect our calculations. The resulting tree-level relations between (pole) masses and Lagrangian parameters are

$$m_{B,4}^2 = g^2 v_4^2 \,, \qquad m_{h,4}^2 = \mu^2 + 3\lambda v_4^2 \,, \qquad m_{\chi,4}^2 = \mu^2 + \lambda v_4^2 \,. \tag{2.5}$$

Before proceeding, we briefly discuss our motivation for studying the Abelian Higgs model. As a Higgs-gauge theory, it shares several key features with realistic models of electroweak phase transitions, including similar scale hierarchies that enable EFT constructions at high temperatures. It also provides a valuable framework for investigating effects related to gauge-fixing, while its relatively small field content simplifies technical calculations, rendering the required operator basis more tractable.

Beyond its aforementioned role in emulating electroweak physics, the Abelian Higgs model has important applications for studying dark-sector phase transitions that are decoupled from the SM [42]. One such example arises from introducing a Yukawa sector at high energies, which could help to explain the recently observed pulsar timing array signals [43, 44]. The Abelian Higgs model also has deep connections to condensed matter physics, where its three-dimensional EFT, the Ginzburg-Landau theory [45], serves as a mean-field description for superconductivity [46–49]. The model is also known to exhibit a tricritical endpoint separating regimes of first-order (type I super conductors) and second-order (type II superconductors) phase transitions. This point was determined non-perturbatively [50] and studied perturbatively in [45, 51]. In contrast to the second-order behavior of the Abelian case, SU(N) models with a scalar in the fundamental representation exhibit only a smooth crossover beyond their critical endpoint [1]. Topological structures in the Abelian Higgs model, such as vortices, were studied in [48, 52, 53]. Such vortices are often used to model cosmic strings [54] studied by large real-time classical field theory simulations [55, 56]. Recently,

JHEP08(2025)109

the classically conformal Abelian Higgs model has been used to predict primordial black holes from supercooled phase transitions [57–59], although their production appears to be smaller than initially expected [60, 61].

3 Dimensional reduction with marginal operators

To study the thermodynamics of a field theory, one must compute its free-energy density, which corresponds to the effective potential evaluated at its global minimum. Our objective, therefore, is to determine the effective potential within perturbation theory. To achieve this, we begin by reviewing the EFT construction of the effective potential, while adding as a novel ingredient the leading marginal operators in the high-temperature expansion.

One major challenge in finite-temperature computations is the emergence of a hierarchy of dynamically generated scales due to in-medium effects. These scales are defined relative to the hard scale πT that sets the typical energy of on-shell particles at high temperatures:

- The *soft (or screening) scale* gT is the characteristic scale of thermal masses and the associated in-medium screening of charged particles. This screening regulates a number of apparent IR divergences in the full theory by giving masses to temporal gauge boson (or temporal scalar) modes.

- The *supersoft scale* $g^{3/2}T$ is the characteristic scale associated with radiatively-induced first-order phase transitions [62–64], which is particularly relevant for perturbative computations of the effective potential.

- The *ultrasoft scale* g^2T is the characteristic scale of the Linde problem [65]. At this scale, sufficiently light bosonic degrees of freedom become strongly coupled and their dynamics confining, ultimately invalidating perturbative expansions.

Fortunately, the confining ultrasoft scale contributes only subdominantly to scalar-driven phase transitions. As a result, purely perturbative descriptions remain viable for sufficiently strong transitions [19, 64], in which the thermally-induced field-dependent mass terms (cf. eq. (3.5)) at the soft scale are large compared to the ultrasoft scale. Thus, while handling the thermal scale hierarchy is a challenge, such a hierarchy is also a prerequisite to generate phase transitions perturbatively [64, 66, 67].

One way to systematically handle the finite-temperature hierarchy in perturbative computations is to use effective field theory techniques [7, 8, 64]. This approach constructs a sequence of effective theories by first integrating out hard-scale contributions, then soft-scale contributions, and finally arriving at a supersoft scale effective theory. In the imaginary-time formalism, the full theory is formulated in four Euclidean dimensions, with a compactified time direction. This compactification leads to a discrete spectrum of allowed energy modes, known as Matsubara frequencies [68]:

$$\omega_n^{\mathrm{B}} = 2n\pi T \qquad \text{for bosons}\,, \tag{3.1}$$

$$\omega_n^{\mathrm{F}} = (2n+1)\pi T \qquad \text{for fermions}\,. \tag{3.2}$$

JHEP08(2025)109

At the soft scale and lower, only bosonic zero modes (with $\omega_n^{\rm B} = 0$) remain dynamical. Consequently, both the soft and supersoft effective theories are defined in a three-dimensional (3d) Euclidean spacetime, with no explicit time dimension.

The initial hard-to-soft EFT is constructed following the standard generic rules used to construct EFTs, by identifying the relevant degrees of freedom and symmetries, and establishing a suitable power-counting scheme [7]. A key ingredient in this step is the high-temperature expansion, since the masses of the surviving scalar and gauge bosons modes must be small compared to the temperature. Integrating out the soft scale is more intricate, as there are two main approaches [64],

$$\mathcal{L}^{\rm 4d} \to \mathcal{L}^{\rm 3d}_{\rm soft} \to \mathcal{L}^{\rm 3d}_{\rm softer} \to V_{\rm eff}^{\rm supersoft}\,, \tag{DR-A}$$

$$\mathcal{L}^{\rm 4d} \to \mathcal{L}^{\rm 3d}_{\rm soft} \to V_{\rm eff}^{\rm supersoft}\,. \tag{DR-B}$$

Henceforth, we will suppress the 3d superscript of the Lagrangians and effective potentials.

In the (DR-A) approach, soft temporal scalar modes are integrated out to obtain an effective description below the soft scale, the *softer* scale, assuming that their Debye mass dominates over field-dependent masses in the Higgs phase. The effective potential is then computed in the Higgs phase by integrating out the spatial gauge boson modes. In contrast, the (DR-B) approach treats temporal and spatial modes on equal footing, integrating them out simultaneously to directly construct the supersoft-scale effective potential. This approach assumes instead that field-dependent masses dominate in the Higgs phase.

In the following, we first construct both the soft and softer EFTs before then detailing how to obtain the resulting EFT-induced supersoft theory.

3.1 Soft scale

The degrees of freedom in the soft effective theory are the zero modes of the Higgs field ϕ, the spatial gauge field B_i, and the temporal gauge field B_0, all of which have mass dimension $[\phi] = [B_i] = [B_0] = \frac{1}{2}$ when normalized canonically. The temporal gauge field, represented by a Lorentz scalar (gauge) singlet, is symmetric under the transformation $B_0 \to -B_0$ while the Higgs boson zero mode exhibits a residual gauge symmetry under purely spatial gauge rotations $\phi \to e^{i\alpha(x)}\phi$, where $\alpha(x)$ is a complex phase. The associated 3d covariant derivative is $D_i = \partial_i - ig_3\, B_i$.

Assuming that $g^4 \ll \lambda \ll g^2$ [66], the leading matching contribution to an operator with n_ϕ Higgs field insertions, n_{B_0} temporal gauge field insertions, and m covariant derivative insertions is

$$\mathcal{L}_{\rm soft} \supset \text{const.} \times \frac{(2\pi T)^3}{8\pi}\Big(\frac{D_i}{2\pi T}\Big)^m \Big(\frac{g\phi}{2\pi T}\Big)^{n_\phi} \Big(\frac{gB_0}{2\pi T}\Big)^{n_{B_0}}\,, \tag{3.3}$$

where the constant prefactor is expected to be of $\mathcal{O}(1)$. This power counting implies that higher-dimensional operators are suppressed by factors of g according to their mass dimension. Up to corrections of $\mathcal{O}(g^8)$, corresponding to dimension-eight operators, the effective 3d Lagrangian at the soft-scale is

$$\begin{aligned}\mathcal{L}_{\rm soft} = {}& \frac{1}{4}F_{ij}F_{ij} + (D_i\phi)^\dagger(D_i\phi) + \mu_3^2\phi^\dagger\phi + \frac{1}{2}(\partial_i B_0)(\partial_i B_0) + \frac{1}{2}m_{\rm D}^2 B_0^2 \\ & + \lambda_3(\phi^\dagger\phi)^2 + h_3(\phi^\dagger\phi)B_0^2 + \kappa_3 B_0^4 + \mathcal{L}^{(6)}_{\rm soft} + \mathcal{O}(g^8)\,,\end{aligned} \tag{3.4}$$

JHEP08(2025)109

where $m_{\rm D}$ is the Debye mass and μ_3^2 the squared effective mass of the scalar field, while λ_3, h_3, and κ_3 are effective coupling constants. In the presence of a 3d background field $v \propto v_4/T^{\frac{1}{2}}$, the effective masses of the zero modes are

$$m_B^2 = g_3^2 v^2\,, \qquad m_h^2 = \mu_3^2 + 3\lambda_3 v^2\,, \qquad m_\chi^2 = \mu_3^2 + \lambda_3 v^2\,, \qquad m_{B_0}^2 = m_{\rm D}^2 + h_3 v^2\,. \tag{3.5}$$

Finally, the term $\mathcal{L}_{\rm soft}^{(6)}$ collects higher-dimensional operators that contribute to correlation functions at $\mathcal{O}(g^6)$. Table 3 in appendix B.2 lists all sixteen allowed operators. Using the field redefinitions detailed in appendix B.2, it is possible to eliminate eight of these operators, which yields the final Lagrangian

$$\begin{aligned}\mathcal{L}_{\rm soft}^{(6)} =& \alpha_{\phi^2F^2} F_{ij}F_{ij}\phi^\dagger\phi + \alpha_{D^2\phi^4}\phi^\dagger\phi(D_i\phi)^\dagger(D_i\phi) + \alpha_{B_0^2F^2}B_0^2F_{ij}F_{ij} + \alpha_{D^2\phi^2B_0^2}\phi^\dagger\phi(\partial_i B_0)^2 \\ &+ \alpha_{B_0^6}B_0^6 + \alpha_{\phi^2B_0^4}(\phi^\dagger\phi)B_0^4 + \alpha_{\phi^4B_0^2}(\phi^\dagger\phi)^2B_0^2 + \alpha_{\phi^6}(\phi^\dagger\phi)^3\,,\end{aligned} \tag{3.6}$$

where the dimension-six Wilson coefficients are denoted by α. The coefficients in eq. (3.4) are known up to $\mathcal{O}(g^4)$, see e.g. [69, 70]. The matching relations for the mass parameters are [70]

$$\begin{aligned}\mu_3^2 =& \mu^2 + \left(\frac{1}{4}g^2 + \frac{1}{3}\lambda\right)T^2 + \frac{\mu^2}{(4\pi)^2}\left(3g^2 - 4\lambda\right)L_b + \delta \\ &+ \frac{T^2}{(4\pi)^2}\left[-\frac{8+39L_b}{36}g^4 + \frac{2(1+3L_b)}{3}g^2\lambda - \frac{10}{3}L_b\lambda^2\right] + \mathcal{O}(g^6)\,,\end{aligned} \tag{3.7a}$$

$$m_{\rm D}^2 = \frac{1}{3}g^2T^2 + \frac{g^2\mu^2}{4\pi^2} + \frac{g^2T^2}{(4\pi)^2}\left[\frac{7-L_b}{9}g^2 + \frac{4}{3}\lambda\right] + \mathcal{O}(g^6)\,. \tag{3.7b}$$

Notably, the expression for the Debye mass is only valid in the high-temperature expansion since at low temperatures $\lim_{T\to 0} m_{\rm D}^2 = \frac{g^2\mu^2}{4\pi^2} \neq 0$. Likewise, the matching relations for the coupling constants are

$$g_3^2 = g^2T - \frac{L_bT}{48\pi^2}g^4 + \mathcal{O}(g^6)\,, \tag{3.7c}$$

$$\kappa_3 = \frac{g^4T}{24\pi^2} + \mathcal{O}(g^6)\,, \tag{3.7d}$$

$$h_3 = g^2T + \frac{T}{(4\pi)^2}\left[\frac{4-L_b}{3}g^4 + 8g^2\lambda\right] + \mathcal{O}(g^6)\,, \tag{3.7e}$$

$$\lambda_3 = \lambda T + \frac{T}{(4\pi)^2}\left[(2-3L_b)g^4 + 6L_bg^2\lambda - 10L_b\lambda^2\right] + \mathcal{O}(g^6)\,, \tag{3.7f}$$

where the quantities

$$L_b \equiv 2\ln\frac{\bar{\Lambda}e^{\gamma_{\rm E}}}{4\pi T}\,, \qquad \delta \equiv \frac{T^2}{(4\pi)^2}\left(c + \ln\frac{3T}{\bar{\Lambda}}\right)\left[-6g^4 + 8g^2\lambda - 8\lambda^2\right]\,, \tag{3.8}$$

encode the dependence on the matching scale $\bar{\Lambda}$,

$$c = \frac{1}{2}\left(\ln\frac{8\pi}{9} + (\ln\zeta_2)' - 2\gamma_{\rm E}\right) \approx -0.124 \tag{3.9}$$

is a dimensionless constant, $\zeta_n \equiv \zeta(n)$ is the Riemann ζ-function with $(\ln\zeta_n)' = \zeta'(n)/\zeta(n)$, and $\gamma_{\rm E}$ is the Euler-Mascheroni constant.

JHEP08(2025)109

We determine the coefficients for the remaining higher dimensional operators in eq. (3.6) by matching to the full theory at one loop; see again appendix B for details. In the following, we focus in particular on the $(\phi^\dagger\phi)^3$ operator, which is the only dimension-six operator contributing to the effective potential at tree-level. Its Wilson coefficient is

$$c_6 = \alpha_{\phi^6} = \frac{\zeta_3}{32\pi^4}\Big(g^6 - \frac{31}{30}g^4\lambda + 5\,g^2\lambda^2 + \frac{20}{3}\lambda^3\Big) + \mathcal{O}(g^8)\,. \tag{3.10}$$

Notably, this expression is gauge-invariant, as expected. This resolves the issue with the naive matching result reported in [24]. Although that work focused on the SM sector, the gauge-dependence issue it identified can also be reproduced in the Abelian Higgs model. The resolution lies in performing appropriate field redefinitions and adopting a physically meaningful operator basis — precisely as anticipated in [24].

None of the Wilson coefficients in eqs. (3.4) and (3.6) run at leading order, because the soft EFT exhibits no one-loop ultraviolet (UV) divergences in dimensional regularization. However, the mass parameter μ_3^2 does run at two loops. In fact, μ_3^2 is the only Wilson coefficient that runs in the super-renormalizable soft theory without marginal operators. The full effect of its running is captured exactly by replacing δ according to [18], such that

$$\delta \to \delta_3 \equiv \frac{1}{(4\pi)^2}\left(c + \ln\frac{3T}{\bar{\Lambda}_{3\mathrm{d}}}\right)\left[-4g_3^4 + 8g_3^2\lambda_3 - 8\lambda_3^2 - 2h_3^2\right], \tag{3.11}$$

where $\bar{\Lambda}_{3\mathrm{d}}$ is the renormalization scale of the soft EFT.

3.2 Softer scale

Next, we integrate out the temporal gauge field B_0, following the conventional approach outlined in [7]. As alluded to in eqs. (DR-A) and (DR-B), this procedure is more nuanced than often acknowledged in the recent literature, with the exception of [25, 64, 71, 72]. We revisit this issue in detail in the next section. We refer to the resulting theory as a softer-scale EFT, rather than an ultrasoft-scale EFT, as the latter is a misnomer, as argued in [64]. The characteristic mass scale for a first-order, scalar-driven phase transition lies above the ultrasoft scale, at the supersoft scale.

One important distinction compared to the soft theory lies in the somewhat more delicate power counting of the softer EFT. Assuming $g_3^4 \ll \lambda_3 \ll g_3^2$, the leading matching contribution to an operator with n Higgs field insertions and m covariant derivatives is given by[2]

$$\mathcal{L}_{\text{softer}} \supset \text{const.} \times \frac{m_{\mathrm{D}}^3}{4\pi}\left(\frac{D_i}{m_{\mathrm{D}}}\right)^m\left(\frac{g_3\phi}{m_{\mathrm{D}}}\right)^n, \tag{3.13}$$

where the constant prefactor is expected to be of $\mathcal{O}(1)$. At first glance, this might suggest that the theory is ill-defined, since higher-dimensional operators are apparently not suppressed

[2]Since $F_{ij} \propto [D_i, D_j]$, insertions of F_{ij} do not need to be accounted for separately. Matching contributions generated at higher-loop level or by diagrams that involve insertions of λ_3, κ_3, or h_3 scale as

$$\mathcal{L}_{\text{softer}} \supset \frac{m_{\mathrm{D}}^3}{4\pi}\left(\frac{2g_3^2}{4\pi m_{\mathrm{D}}}\right)^{\ell-1}\left(\frac{2\lambda_3}{g_3^2}\right)^{n_\lambda}\left(\frac{h_3}{g_3^2}\right)^{n_h}\left(\frac{12\kappa_3}{g_3^2}\right)^{n_\kappa}\left(\frac{D_i}{m_{\mathrm{D}}}\right)^m\left(\frac{g_3\phi}{m_{\mathrm{D}}}\right)^n, \tag{3.12}$$

where ℓ is the considered loop order using n_λ insertions of λ_3, n_h insertions of h_3, and n_κ insertions of κ_3.

JHEP08(2025)109

by powers of g_3 compared to super-renormalizable ones. However, when computing vacuum diagrams in the symmetric phase, each additional vertex from an operator (3.13) introduces a suppression

$$\left(\frac{g_3^2}{4\pi\bar{\mu}_3}\right)^{\frac{n}{2}}\left(\frac{\bar{\mu}_3}{m_{\rm D}}\right)^{n+m-3} \propto \left(\frac{1}{16\pi^2 y}\right)^{\frac{n}{4}}\left(3g^2 y\right)^{\frac{n+m-3}{2}}, \tag{3.14}$$

where $\bar{\mu}_3 \ll m_{\rm D}$ is the effective Higgs mass parameter and $\bar{y} \equiv \bar{\mu}_3^2/\bar{g}_3^4$. This means that the theory can be used to compute the effective potential in the symmetric phase if

$$(3g^2)^{-1} \gg \bar{y} \gg (4\pi)^{-2}\,. \tag{3.15}$$

The situation is more complex in the broken phase since the Higgs condensate can generate contributions to the spatial gauge boson and Higgs masses that disrupt the validity of the power counting for strong phase transitions. This imposes additional consistency constraints, similar to those in eq. (3.15). These constraints are analyzed in detail in sections 3.3 and 4.2.

In practice, we construct the softer effective theory using the same process as in section 3.1. By again including operators up to dimension six and using field redefinitions to then eliminate redundant operators, we obtain the Lagrangian

$$\begin{aligned}\mathcal{L}_{\rm softer} = &\frac{1}{4}F_{ij}F_{ij} + (\overline{D}_i\phi)^\dagger(\overline{D}_i\phi) + \bar{\mu}_3^2\phi^\dagger\phi + \bar{\lambda}_3\,(\phi^\dagger\phi)^2 + c_6\,(\phi^\dagger\phi)^3 \\ &+ \overline{\alpha}_{D^2\phi^4}\,\phi^\dagger\phi(\overline{D}_i\phi)^\dagger(\overline{D}_i\phi) + \overline{\alpha}_{\phi^2F^2}\,F_{ij}F_{ij}\phi^\dagger\phi\,,\end{aligned} \tag{3.16}$$

where $\overline{D}_i = \partial_i - i\bar{g}_3 B_i$ is the effective covariant derivative, $\bar{g}_3$ its associated gauge coupling, and $\bar{\lambda}_3$ is the quartic Higgs self-interaction. The corresponding effective masses are the ones from eq. (3.5) adapted to the softer Lagrangian (3.16). After matching at one loop, the gauge coupling $\bar{g}_3 = g_3$ is the same as in the soft scale theory, while $\bar{\lambda}_3$ is given as [69]

$$\bar{\lambda}_{3,\rm red} = \frac{\bar{\lambda}_3}{4\pi m_{\rm D}} = \lambda_{\rm red} - \left(1 + \frac{\mu_3^2}{6m_{\rm D}^2}\right)\frac{h_{\rm red}^2}{2} + \mathcal{O}(g^4)\,, \tag{3.17}$$

where

$$h_{\rm red} = \frac{h_3}{4\pi m_{\rm D}}\,, \qquad \kappa_{\rm red} = \frac{\kappa_3}{4\pi m_{\rm D}}\,, \qquad \lambda_{\rm red} = \frac{\lambda_3}{4\pi m_{\rm D}}\,, \tag{3.18}$$

are the relevant effective expansion parameters of the soft theory. Analogously to the soft theory, the mass parameter $\bar{\mu}_3^2$ is the only UV divergent Wilson coefficient in the super-renormalizable theory without marginal operators. To ensure that its running is consistent with that of μ_3^2, a two-loop matching is required, leading to the expression

$$\bar{\mu}_3^2 = \mu_3^2 - m_{\rm D}^2 h_{\rm red} - m_{\rm D}^2 h_{\rm red}^2\left[1 + 2\ln\frac{\bar{\Lambda}_{3\rm d}}{2m_{\rm D}}\right] + 6m_{\rm D}^2 h_{\rm red}\kappa_{\rm red} + \mathcal{O}(g^5)\,, \tag{3.19}$$

where the last term is of $\mathcal{O}(g^6)$, which is already of the order of hard three-loop contributions to the scalar mass, while the soft three-loop contribution is of $\mathcal{O}(g^5)$. The result in eq. (3.19)

JHEP08(2025)109

is readily obtained using `DRalgo` [73] or partially available in [69]. The dimension-six Wilson coefficients at one loop,

$$\overline{\alpha}_{\phi^2F^2} = \alpha_{\phi^2F^2} + \mathcal{O}(g^2)\,, \tag{3.20a}$$

$$\overline{\alpha}_{D^2\phi^4} = \alpha_{D^2\phi^4} - 4\pi\frac{h_{\rm red}^2}{12m_{\rm D}} + \mathcal{O}(g^2)\,, \tag{3.20b}$$

$$\overline{\alpha}_{\phi^6} = \alpha_{\phi^6} + (4\pi)^2\frac{h_{\rm red}^2}{6}\,(h_{\rm red} - \lambda_{\rm red}) + \mathcal{O}(g^4)\,, \tag{3.20c}$$

were determined in appendix C. Written in terms of g and λ, one has

$$\bar{c}_6 = \alpha_{\phi^6} + \frac{\sqrt{3}\,g^3}{8\pi}\Big(\frac{m_{\rm D}^{\rm LO}}{m_{\rm D}}\Big)^3(1 - x_{\rm LO}) + \mathcal{O}(g^4)\,, \tag{3.21}$$

where we used the leading-order (LO) results of $x_{\rm LO} = \frac{\lambda}{g^2}$ and $m_{\rm D}^{\rm LO} = \frac{gT}{\sqrt{3}}$. As generally expected from eq. (3.13), the leading non-vanishing contribution to $\overline{\alpha}_{\phi^6}$ appears at $\mathcal{O}(g^3)$, while higher-order corrections to the Debye mass $m_{\rm D}$ become important at $\mathcal{O}(g^5)$. In the following sections, when discussing the phase transition dynamics, we also require the combination

$$\bar{x} \equiv \frac{\bar{\lambda}_3}{\bar{g}_3^2} = x_{\rm LO} - \frac{\sqrt{3}\,g}{8\pi}\Big(\frac{m_{\rm D}^{\rm LO}}{m_{\rm D}}\Big)\Big(1 + \frac{\mu_3^2}{6m_{\rm D}^2}\Big) + \mathcal{O}(g^2)\,. \tag{3.22}$$

It is this quantity, the ratio of thermal scalar self-coupling to thermal gauge coupling, that controls the strength of a phase transition.

3.3 Supersoft scale effective potential

Before focusing on the thermodynamics, we first detail the regimes of validity for the two EFT setups (DR-A) and (DR-B). To this end, we consider the effective potential; see also [69, 70] for a more detailed derivation or [64] for further qualitative details.

In gauge-Higgs theories, and in particular in the Abelian Higgs model, radiative corrections generically induce a barrier between the local minima of the effective potential. Therefore, it is necessary to inspect these corrections to correctly describe first-order transitions. In general, the leading contributions are generated by spatial and temporal gauge boson modes, while the Higgs contributions are subdominant. Working within the soft scale EFT, and expressing the effective potential in terms of the 3d background field v, one has

$$\Delta V_{\rm tree} = \frac{1}{2}\mu_3^2v^2 + \frac{1}{4}\lambda_3v^4 + \frac{1}{8}c_6v^6\,, \tag{3.23a}$$

$$\Delta V_{\rm 1loop,gauge} = -\frac{1}{12\pi}\Big(2m_B^3 + m_{B_0}^3\Big) = -\frac{1}{12\pi}\Big(2g_3^3v^3 + (m_{\rm D}^2 + h_3v^2)^{\frac{3}{2}}\Big)\,, \tag{3.23b}$$

where $\Delta V(v) = V(v) - V(0)$, while m_B is the spatial and m_{B_0} the temporal gauge boson mass defined in eq. (3.5). Notably, c_6 is the only marginal operator coefficient that contributes to the tree-level potential, while all other coefficients only contribute at one-loop. Their effect remains subdominant compared to the leading contributions from gauge fields and is therefore omitted here. Additionally, since λ_3 is positive, the tree-level potential does not exhibit a barrier between its minima; cf. [22].

JHEP08(2025)109

If there is no hierarchy between $m_{\rm D}^2$ and Higgs contribution to the temporal gauge boson mass $h_3 v^2$, one has to use the (DR-B) setup. The leading-order effective potential is given by the sum of tree-level and one-loop gauge field contributions,

$$\begin{aligned}\Delta V_{\rm soft} &= \Delta V_{\rm tree} + \Delta V_{\rm 1loop,gauge} \\ &= \frac{1}{2}\mu_3^2 v^2 + \frac{1}{4}\lambda_3 v^4 + \frac{1}{8}c_6 v^6 - \frac{1}{12\pi}\Big(2g_3^3 v^3 + (m_{\rm D}^2 + h_3 v^2)^{\frac{3}{2}}\Big)\,. \end{aligned} \tag{3.24}$$

A hierarchy $m_{\rm D}^2 \gg h_3 v^2$ allows for constructing an EFT at the softer scale by integrating out the temporal mode using the (DR-A) setup. In this approach, soft contributions are perturbatively absorbed into the Wilson coefficients of the softer theory. This corresponds to an expansion in $h_3 v^2/m_{\rm D}^2$, or equivalently, using leading-order (hard-scale) matching relations, an expansion in $3\,v^2/T$, where the factor 3 results from the definition of the Debye mass. Consequently, the softer EFT is only valid for relatively weak transitions, where $v^2/T \sim v_4^2/T^2 \ll 1/3$. On the other hand, the softer EFT setup is not suitable for describing strong phase transitions with large field-induced mass contributions.[3] In section 4, we specifically demonstrate this by showing that for very strong transitions, higher-dimensional operators become dominant when contributions from the soft temporal sector are properly accounted for.

The soft to softer EFT matching relations (3.17), (3.19), and (3.20) follow from the series expansion of last term in eq. (3.23b). However, the tree-level potential within the softer EFT does not have a barrier, which is again generated by radiative corrections. By including one-loop contributions generated by the spatial gauge boson modes, one obtains the leading-order effective potential

$$\Delta V_{\rm softer} = \frac{1}{2}\bar{\mu}_3^2 v^2 + \frac{1}{4}\bar{\lambda}_3 v^4 + \frac{1}{8}\bar{c}_6 v^6 - \frac{1}{6\pi}\bar{g}_3^3 v^3\,. \tag{3.25}$$

Conversely, while there is in principle no reason to presume a hierarchy between $m_{\rm D}^2$ and $h_3 v^2$ in the soft theory setup, a reasonable estimate of the effective potential for strong transitions, where $h_3\, v^2 \gtrsim m_{\rm D}$, can be obtained by setting $m_{\rm D}^2 \to 0$ in eq. (3.24). In this limit, one obtains

$$\Delta V_{\rm soft}^{\mathcal{E}} = \Delta V_{\rm soft}\big|_{m_{\rm D}^2 \ll h_3 v^2} = \frac{1}{2}\mu_3^2 v^2 + \frac{1}{4}\lambda_3 v^4 + \frac{1}{8}c_6 v^6 - \frac{v^3}{6\pi}\Big(g_3^3 + \frac{1}{2}h_3^{3/2}\Big)\,, \tag{3.26}$$

where the so-called enhancement factor $\mathcal{E}$ is defined in eq. (3.34). While this approximation is relatively crude, it works reasonably well in the regime where v becomes large enough for the high-temperature expansion to start breaking down. For a more detailed discussion, see section 4.3. One key advantage of using the approximation is that it allows for an analytical estimate of the latent heat at the critical temperature in the (DR-B) setup. Inspecting

[3] For a generic SU(N) gauge-scalar theory with N_t scalars in the adjoint and N_d scalars in the fundamental representation, as well as $N_{\rm f}$ fermionic degrees of freedom, a similar argument leads to $v^2/T \ll \frac{2}{3}N + \frac{2}{3}N_t + \frac{1}{3}N_d + \frac{1}{6}N_{\rm f}$. Due to the large number of fermions with a high degree of internal symmetry, the fermionic contribution can render the Debye mass large and hence increase the range of validity for a softer EFT. For example, in the SM $N_{\rm f} = 3(1 + N_{\rm c})$ for 3 generations of both lepton and $N_{\rm c} = 3$ quark doublets, which leads to $v^2/T \ll \frac{11}{3}$ using $N = 2$, $N_d = 1$, $N_t = 0$. For non-perturbative studies that explicitly retain the temporal mode in the lattice action, see e.g. [74, 75].

JHEP08(2025)109

eq. (3.26), we see that the temporal mode effectively enhances the cubic term. Indeed, utilizing leading-order (hard-scale) matching relations [76], one obtains

$$-T\frac{v^3}{6\pi}\Big(g_3^3+\frac{1}{2}h_3^{3/2}\Big)=-Tv_4^3\frac{g^3}{12\pi}\Big((2)_{\text{spatial}}+(1)_{\text{temporal}}\Big)+\mathcal{O}(g^4)\,. \tag{3.27}$$

In the limit where the field-dependent contribution dominates over the Debye mass, the temporal mode gives a 50% *soft-scale enhancement* to the cubic term. Therefore, temporal modes are expected to further increase the strength of already strong transitions that push the high-temperature expansion to its limits.

Since the effective potential, due to its mass dimension being $[\Delta V]=3$, exhibits a trivial T^3 scaling, it is practical to define dimensionless potentials when computing thermodynamic quantities

$$\Delta\widetilde{V}(\varphi,\omega_q)\equiv\frac{\Delta V(v)}{\omega_q^3}\,,\qquad\qquad \varphi^2=\frac{v^2}{\omega_q}\,, \tag{3.28}$$

where $\omega_q\propto T$ is some characteristic energy scale. One convenient choice is to identify ω_q with the square of the gauge coupling that sets the size of the cubic v^3 term (i.e. the size of the potential barrier separating the local minima), so that

$$\omega_q=\begin{cases} g_3^2 & \text{full soft potential (3.24)}\\ \bar{g}_3^2 & \text{full softer potential (3.25)}\\ g_{\text{eff}}^2 & m_{\text{D}}^2\ll h_3v^2 \text{ potential (3.26)}\end{cases}\,,\qquad g_{\text{eff}}^3=g_3^3+\frac{1}{2}h_3^{\frac{3}{2}}\approx\frac{3}{2}g_3^3\,. \tag{3.29}$$

In this convention, the corresponding rescaled effective potentials associated with at leading order effective potentials of (3.24)–(3.26) share the same overall shape

$$\Delta\widetilde{V}(\varphi,A,B,C,D)\equiv\frac{A}{2}\varphi^2+\frac{B}{4}\varphi^4+\frac{C}{8}\varphi^6-\frac{1}{6\pi}\varphi^3-\frac{1}{12\pi}\Big(D+\varphi^2\Big)^{\frac{3}{2}}\,, \tag{3.30}$$

where the size of the φ^3 term is not a free parameter but fixed by the normalization. Explicitly, they are given as

$$\Delta\widetilde{V}_{\text{softer}}=\frac{\bar{y}}{2}\varphi^2+\frac{\bar{x}}{4}\varphi^4+\frac{\bar{c}_6}{8}\varphi^6-\frac{1}{6\pi}\varphi^3\,, \tag{3.31a}$$

$$\Delta\widetilde{V}_{\text{soft}}=\frac{y}{2}\varphi^2+\frac{x}{4}\varphi^4+\frac{c_6}{8}\varphi^6-\frac{1}{6\pi}\varphi^3-\frac{1}{12\pi}(y_{\text{D}}+\varphi^2)^{\frac{3}{2}}\,, \tag{3.31b}$$

$$\Delta\widetilde{V}_{\text{soft}}^{\mathcal{E}}=\Delta\widetilde{V}_{\text{soft}}\big|_{y_{\text{D}}\ll\varphi^2}=\frac{y}{2}\varphi^2+\frac{x}{4}\varphi^4+\frac{c_6}{8}\varphi^6-\frac{1}{6\pi}\varphi^3\,, \tag{3.31c}$$

where we have defined the dimensionless quantities

$$x=\frac{\lambda_3}{\omega_q}\,,\qquad\qquad \bar{x}=\frac{\overline{\lambda}_3}{\omega_q}\,, \tag{3.32a}$$

$$y=\frac{\mu_3^2}{\omega_q^2}\,,\qquad\qquad \bar{y}=\frac{\bar{\mu}_3^2}{\omega_q^2}\,,\qquad\qquad y_{\text{D}}=\frac{m_{\text{D}}^2}{\omega_q^2}\,. \tag{3.32b}$$

Notice, that the quantities x and y in the rescaled full soft potential (3.31b) are not the same as the x and y in the approximated potential (3.31c), as the two potentials are

JHEP08(2025)109

defined using different choices of ω_q to reflect the effective enhancement of the cubic term. In general, if the size of the cubic term in the *original* potential $\Delta V(v)$ is rescaled by some factor $\mathcal{E}$, this leads to a corresponding rescaling

$$\omega_q \to \mathcal{E}^{\frac{2}{3}}\omega_q\,, \qquad x \to \mathcal{E}^{-\frac{2}{3}}x\,, \qquad y \to \mathcal{E}^{-\frac{4}{3}}y\,. \tag{3.33}$$

In our case, the effective height of the barrier in the original approximated potential (3.26) is enhanced by a factor

$$\mathcal{E} = \frac{g_{\rm eff}^3}{g_3^3} \approx \frac{3}{2}\,, \tag{3.34}$$

compared to the barrier in the softer potential (3.25) due to the impact of temporal gauge modes. We expect that this enhancement is of the same order for general SU(N) theories with one fundamental scalar.

To summarize, within our perturbative description of the Abelian Higgs model effective potential, the supersoft scale is always the characteristic scale associated with first-order phase transitions. We have constructed two approximations eqs. (3.25) and (3.26) for the LO potential eq. (3.24), corresponding to two limits, for relatively weak and strong transitions, respectively. These approximations arise from how one treats the temporal mode. We remark that the latter construction for strong transitions, where the temporal mode is not integrated out to construct a softer EFT, has indeed been applied in recent work [25, 72] in the context of other models, and analogous constructions can be obtained using the Higgs effective field theory (HEFT) functionalities in `HEFT.m` of `DRalgo` [73] for generic models. See also [77] for a recent application of `DRalgo`.

We emphasize that constructing the supersoft scale effective potential is qualitatively different from the matching computations used to compute the Wilson coefficients in the soft and softer EFTs, which are performed in the symmetric phase with $v = 0$. In contrast, the supersoft scale effective potential is constructed only in the Higgs phase around a non-vanishing scalar background. In the Higgs phase, in addition to the temporal gauge field mode, also the spatial gauge field modes are soft and hence integrated out to construct the effective potential [63, 64, 76].

4 Phase transition thermodynamics

The free energy, or equivalently the pressure $p(T)$, governs the behavior of systems in thermal equilibrium. In particular, the pressure determines the strength of a phase transition, which is often characterized in terms of the parameter

$$\alpha \equiv \frac{\Delta\theta}{3\omega_+}\,, \tag{4.1}$$

where $\Delta\theta = \theta_+ - \theta_-$ is the discontinuity of the pseudo trace anomaly $\theta_\pm = e - p/c_s^2$ [78, 79] across the transition, $\omega = e + p$ the enthalpy, $e = T\partial_T p - p$ the energy density, and c_s the speed of sound in the plasma. The subscript $\pm$ specifies that a quantity is evaluated in either the high- or low-temperature phase, while the normalization factor 3 ensures that α is consistent with the definition in the bag model [79]. In general, the speed of sound

JHEP08(2025)109

c_s is also determined by the pressure, but for our purposes below it is sufficient to use the leading-order result $c_s^2 = 1/3$ [80]. We likewise use the leading result for the pressure in the high-temperature phase,

$$p_+ = g_\star \frac{\pi^2}{90} T^4 + \mathcal{O}(g^2 T^4)\,, \tag{4.2}$$

where $g_\star = g_{\mathrm{DS},\star} = 4$ is the effective number of relativistic degrees of freedom in the dark sector (DS) Abelian Higgs model. This represents a simplification, as we do not include the full number of relativistic degrees of freedom in the SM. In principle, the total effective number should account for both the SM and the dark sector [17], leading to $g_{\mathrm{tot},\star} = g_{\mathrm{SM},\star} + g_{\mathrm{DS},\star}\,\xi_{\mathrm{D}}^4$, where $\xi_{\mathrm{D}} \equiv T_{\mathrm{DS}}/T_{\mathrm{SM}}$ accounts for a possible temperature difference between the two sectors [81, 82].

The pressure in the low-temperature or Higgs phase is

$$p(T) = p_+ - T\Delta V(v_{\mathrm{min}})\,, \qquad \Delta V(v_{\mathrm{min}}) = \omega_q^3 \Delta\widetilde{V}(\varphi_{\mathrm{min}})\,, \qquad v_{\mathrm{min}}^2 = \omega_q \varphi_{\mathrm{min}}^2\,, \tag{4.3}$$

where $\Delta\widetilde{V}(\varphi)$ is the rescaled supersoft scale effective potential defined in section 3.3, ω_q the corresponding normalization scale, and $v_{\mathrm{min}}(T)$ the value of the background field that minimizes the potential. Above the critical temperature T_{c}, the origin $v_{\mathrm{min}} = 0$ is the global minimum of the effective potential. For smaller temperatures, the global minimum shifts to a finite value $v_{\mathrm{min}} \neq 0$ that is separated from the now local minimum at the origin by a potential barrier. Directly at the critical temperature, the two minima are degenerate, so that $\Delta V(v_{\mathrm{min}}) = 0$. Using the definition (4.1), one obtains the relation

$$\alpha \approx \frac{1}{3\,\partial_T p_+}\Big(T\frac{\mathrm{d}}{\mathrm{d}T} - 3\Big)\Delta V = \frac{30}{(2\pi)^2 g_\star} T\frac{\mathrm{d}}{\mathrm{d}T}\Big(\frac{\omega_q^3}{T^3}\Delta\widetilde{V}\Big)\,, \tag{4.4}$$

which we use going forward.

4.1 Leading-order effective potentials

To proceed, one must provide a suitable expression for the effective potential. Following the discussion in section 3.3, this can be achieved through different approaches, resulting in at least two potentially viable EFT constructions: the (DR-A) or (DR-B) setups. We now discuss each setup separately.

Softer-induced effective potential. In the (DR-A) EFT setup, the effective potential is constructed by first integrating out the temporal scalar before addressing the spatial gauge boson modes. At leading order in the super-renormalizable theory, one obtains the expression given in [76]. Following [76], it is straightforward to add higher-order perturbative corrections to the effective potential. We do not consider them in this work, but instead investigate the impact of the leading correction due to the marginal operator $(\phi^\dagger\phi)^3$, which yields the effective potential (3.25) and the associated rescaled potential

$$\Delta\widetilde{V}_{\mathrm{softer}} = \frac{\bar{y}}{2}\varphi^2 + \frac{\bar{x}}{4}\varphi^4 + \frac{\bar{c}_6}{8}\varphi^6 - \frac{1}{6\pi}\varphi^3\,, \qquad \omega_q = \bar{g}_3^2\,, \tag{4.5}$$

JHEP08(2025)109

which we have already defined in (3.31a). The field value $\varphi_{\min}$ that minimizes the rescaled potential is a function of the dimensionless parameters $\bar{y}$, $\bar{x}$, and $\bar{c}_6$. Using that $\bar{g}_3^2/T$, $\bar{x}$, and $\bar{c}_6$, are temperature independent at leading order [17], cf. also eqs. (3.7), (3.21), and (3.22), one can simplify the expression for the transition strength of eq. (4.4) by using the chain rule

$$T\frac{\mathrm{d}}{\mathrm{d}T}\Big(\frac{\Delta V(\varphi_{\min})}{T^3}\Big) \approx \frac{\bar{g}_3^6\eta_{\bar{y}}}{T^3}\partial_{\bar{y}}\Delta\widetilde{V}(\varphi_{\min})\,, \qquad \eta_{\bar{y}} \equiv T\frac{\mathrm{d}\bar{y}}{\mathrm{d}T}\,. \tag{4.6}$$

At leading order (without including higher-order loop corrections), the derivative $\partial_{\bar{y}}\Delta\widetilde{V}$ is just $\varphi_{\min}^2$, which yields the final result

$$\alpha(T) \approx \frac{15}{(2\pi)^2 g_\star}\frac{\bar{g}_3^6\eta_{\bar{y}}}{T^3}\varphi_{\min}^2\,. \tag{4.7}$$

We emphasize that this expression is only valid at leading order. At higher orders, it is the jump in the 3d scalar condensate [30]

$$\Delta\langle\phi^\dagger\phi\rangle \equiv \frac{\mathrm{d}}{\mathrm{d}\bar{\mu}_3^2}\Delta V = \bar{g}_3^2\partial_{\bar{y}}\Delta\widetilde{V}(\varphi_{\min})\,, \tag{4.8}$$

that contributes to α.[4] At the critical temperature, where $\Delta\widetilde{V} = 0$ must hold, it is possible to give an analytic expression for the Higgs phase minimum, which is located at

$$\varphi_{\min} = \frac{\overline{\mathcal{F}}_+ - \overline{\mathcal{F}}_-}{2\pi\bar{x}\sqrt{\bar{r}}}\,, \qquad \overline{\mathcal{F}}_\pm \equiv \Big(\sqrt{1+\bar{r}} \pm \sqrt{\bar{r}}\Big)^{\frac{1}{3}}\,, \qquad \bar{r} = \frac{3}{(2\pi)^2}\frac{\bar{c}_6}{\bar{x}^3}\,. \tag{4.9}$$

For $\bar{y}_{\mathrm{c}}$, one likewise obtains

$$\bar{y}_{\mathrm{c}} = \frac{(\overline{\mathcal{F}}_+ - \overline{\mathcal{F}}_-)^2(\overline{\mathcal{F}}_+^2 + \overline{\mathcal{F}}_-^2)}{(4\pi)^2\bar{x}\,\bar{r}} = \frac{1}{2}\bar{x}\,\varphi_{\min}^2\frac{(\overline{\mathcal{F}}_+^2 + \overline{\mathcal{F}}_-^2)}{2}\,. \tag{4.10}$$

When neglecting the impact of the sextic operator, these expressions reduce to the well-known limit

$$\varphi_{\min} = \frac{1}{3\pi\bar{x}}\,, \qquad \bar{y}_{\mathrm{c}} = \frac{1}{18\pi^2\bar{x}}\,. \tag{4.11}$$

This result implies that the strength of the phase transition scales as $\varphi_{\min}^2 \propto \bar{x}^{-2}$, while including higher-dimensional operators is most relevant for large values of $\bar{r}$, which scales as $\bar{x}^{-3}$. In other words, small values of $\bar{x}$ characterize the region of parameter space with both the strongest transitions and the largest impact of higher-dimensional operators.

Soft-induced effective potential. Conversely, if the effective potential is computed by treating temporal scalars and spatial gauge boson modes on equal footing, following the (DR-B) setup, the leading-order potential — including the sextic operator — is given by eq. (3.24). The associated rescaled potential is

$$\Delta\widetilde{V}_{\mathrm{soft}} \equiv \frac{y}{2}\varphi^2 + \frac{x}{4}\varphi^4 + \frac{c_6}{8}\varphi^6 - \frac{1}{12\pi}\Big(2\varphi^3 + (y_{\mathrm{D}} + \varphi^2)^{\frac{3}{2}}\Big)\,, \qquad \omega_q = g_3^2\,, \tag{4.12}$$

[4] Calculation in terms of the condensate can be made manifestly gauge-invariant order by order, by applying strict expansion around the leading-order minimum. The leading-order result in eq. (4.7) is also gauge invariant, since the minimum of the leading-order potential does not depend on the gauge fixing parameter.

JHEP08(2025)109

which we have already defined in (3.31b). In analogy to the (DR-A) setup, the minimum of the rescaled potential $\varphi_{\min}$ depends on $y_{\rm D}$, y, x, and c_6, where y is the only parameter that is temperature dependent at leading order. This gives

$$\alpha(T) \approx \frac{15}{(2\pi)^2 g_\star} \frac{g_3^6 \eta_y}{T^3} \varphi_{\min}^2 \,, \qquad\qquad \eta_y \equiv T \frac{\mathrm{d}y}{\mathrm{d}T} \approx \eta_{\bar{y}} \,. \tag{4.13}$$

This expression is the same as eq. (4.7), expect that it contains g_3 in place of $\bar{g}_3$ and that $\varphi_{\min}$ now minimizes soft-induced potential (4.12) instead of the softer-induced one given in eq. (4.5). Hence, the main difference between the (DR-A) and (DR-B) approaches is the predicted location of the minimum.

Due to the non-analytic structure of the potential (4.12), it is quite challenging to find an analytic expression for $\varphi_{\min}$. However, as discussed in section 3.3, we may estimate the potential for strong transitions by setting $y_{\rm D} \to 0$, which yields the rescaled effective potential (3.31c). This potential is formally of the same shape as the softer-induced effective potential (3.31a), allowing us to derive an analytic estimate for the minimum at $T_{\rm c}$. To obtain the correct result, it is however important to remember that the potential (3.31c) is defined using a normalization scale $\omega_q = g_{\rm eff}^2$ that differs from the scale $\omega_q = g_3^2$ of the full soft potential (4.12). This impacts the definition of x and y as well as the location of the minimum $\varphi_{\min}$. Using the replacements (3.33) and $\varphi_{\min} \to \varphi_{\min}/\mathcal{E}^{\frac{1}{3}}$ to account for the change in ω_q, we find the minimum

$$\varphi_{\min} \approx \mathcal{E} \times \frac{\mathcal{F}_+ - \mathcal{F}_-}{2\pi x \sqrt{r}} \,, \qquad \mathcal{F}_\pm \equiv \left(\sqrt{1+r} \pm \sqrt{r}\right)^{\frac{1}{3}} \,, \qquad r = \mathcal{E}^2 \times \frac{3}{(2\pi)^2} \frac{c_6}{x^3} \,, \tag{4.14}$$

where $x = \lambda_3/g_3^2$ is defined as usual. The quantity $\mathcal{E} = 3/2$ was already defined in (3.34) and parametrizes the enhancement of the transition strength due to temporal gauge boson modes. The corresponding soft-enhanced critical $y_{\rm c}$ is

$$y_{\rm c} = \mathcal{E}^2 \frac{(\mathcal{F}_+ - \mathcal{F}_-)^2 (\mathcal{F}_+^2 + \mathcal{F}_-^2)}{(4\pi)^2 x\, r} = \frac{1}{2} x\, \varphi_{\min}^2 \frac{(\mathcal{F}_+^2 + \mathcal{F}_-^2)}{2} \,. \tag{4.15}$$

When neglecting the impact of the sextic operator, one finds the limit

$$\varphi_{\min} = \frac{\mathcal{E}}{3\pi x} \,, \qquad\qquad y_{\rm c} = \frac{\mathcal{E}^2}{18\pi^2 x} \,. \tag{4.16}$$

As in the (DR-A) setup, small values of x characterize the region with both strong transitions and the largest impact of higher dimensional operators. Therefore, our analysis will primarily focus on the regime of small x-values.

4.2 EFT consistency at the critical temperature

Qualitatively, small values of x and $\bar{x} \sim x$ yield strong phase transitions because they correspond to large values of the background field $\varphi_{\min} \sim x^{-1}$. In section 3.3, we already discussed how the high-temperature expansion and with it consistency of the EFT description breaks down for sufficiently large values of $\varphi_{\min}$ (or equivalently, small values of x). On the other hand, it is well known that the thermal EFTs remain consistent but become

JHEP08(2025)109

non-perturbative for large values of x [1, 52, 83]. In the softer theory, this non-perturbative behavior is often related to the existence of a critical endpoint for the transition, which is characterized by a divergent correlation length that is said to signal the associated breakdown of perturbation theory. For the Abelian Higgs model it is located at $\bar{x}_c \approx 0.28$ [50]. The existence of this endpoint is not readily apparent in perturbation theory and is thus typically investigated using lattice or other non-perturbative methods.

In this section, we quantitatively examine constraints on the consistency and perturbativity of the soft and softer EFTs. One particular focus is the impact of higher-dimensional operators in the regime close to the eventual breakdown of the high-temperature expansion. For each EFT introduced in section 3, we examine (i) the power counting that is used to construct the EFT by truncating the infinite tower of higher-dimensional operators that contribute to it in principle, and (ii) the perturbative power counting that underlies the loop expansion within the EFT. It is important to emphasize that these are two independent considerations:

(i) *Validity of power counting*:
if the truncation of higher-dimensional operators is invalid, the resulting effective theory becomes inconsistent, as it would require accounting for the entire tower of effective interactions even at leading order. In the soft and softer EFTs, this signals the breakdown of the high-temperature expansion and the EFT cannot be applied to compute observables.

(ii) *Perturbativity of the loop expansion*:
if the power counting holds but the loop expansion fails, the EFT remains consistent but becomes non-perturbative. In this case, non-perturbative methods like lattice simulations are needed to compute thermodynamic quantities such as $\alpha(T)$.

One important factor in the context of the soft and softer EFTs is that non-perturbative behavior propagates upwards through the chain of effective theories. Therefore, if the softer EFT is non-perturbative, then so is the soft EFT; and if the soft EFT is non-perturbative, then so is the full theory.

(i) Consistency.

In the symmetric phase, the power counting (3.3) ensures that the soft-scale EFT is consistent as long as the coupling constants in the full theory are perturbative,

$$\lambda, g^2 \ll (4\pi)^2 \,. \tag{4.17}$$

The power counting for the softer theory is more subtle, and only consistent if condition (3.15) is satisfied. Working at the critical temperature T_c and using $y_c \approx \frac{1}{18\pi^2\bar{x}}$, this gives the further constraint

$$\frac{g^2}{6\pi^2} \approx 0.017 g^2 \ll \bar{x} \ll \frac{8}{9} \,. \tag{4.18}$$

In the broken phase, the Higgs mechanism generates additional mass contributions to the effective masses of the Higgs boson, the spatial gauge boson modes, and the temporal gauge

JHEP08(2025)109

boson modes which can spoil the consistency of the EFT power counting. The most stringent constraint turns out to be associated with the mass of the spatial gauge boson modes,

$$m_B = g_3 v = g v_4 \big(1 + \mathcal{O}\left(g^2\right)\big) \ . \tag{4.19}$$

To ensure consistency of the soft theory in the broken phase, this mass has to be small compared to the hard-scale πT. Working at the critical temperature T_c and using $v \approx \frac{\mathcal{E} g_3}{3\pi x}$, this yields the constraint

$$\frac{\mathcal{E} g^2}{3\pi^2} \approx 0.051\, g^2 \ll x \ . \tag{4.20}$$

Since the leading contribution to the effective potential from higher-dimensional operators in the soft theory scales as

$$V_{\text{soft}} \supset \pi^2 T^3 \Big(\frac{gv}{2\pi T}\Big)^{2n} , \tag{4.21}$$

this condition also ensures that contributions from higher-dimensional operators are suppressed compared to those from super-renormalizable operators.

To also ensure consistency of the softer theory, m_B has to be small compared to the Debye mass $m_{\text{D}} \approx \frac{gT}{\sqrt{3}}$. Working at the critical temperature T_c and using $v \approx \frac{\bar{g}_3}{3\pi \bar{x}}$, this gives the constraint

$$\frac{\sqrt{3}}{3\pi} g \approx 0.18\, g \ll \bar{x} \ . \tag{4.22}$$

The leading contribution to the effective potential from higher-dimensional operators in the softer theory scales as

$$\Delta V_{\text{softer}} \supset \frac{m_{\text{D}}^3}{4\pi} \Big(\frac{g_3 v}{m_{\text{D}}}\Big)^{2n} \ . \tag{4.23}$$

Thus, as in the soft case, eq. (4.22) also ensures that higher-dimensional operator contributions remain subdominant, provided the effective theory is consistent from the outset.

(ii) Perturbativity.

In general, thermal field theories are non-perturbative if they contain light bosons with masses that are not much larger than the relevant non-perturbative scale associated with the Linde IR problem. Since particles are generally heavier in the broken phase than in the symmetric phase, the resulting constraints are more stringent in the symmetric phase. Furthermore, non-perturbative behavior in the softer theory implies that the soft theory is also non-perturbative. Therefore, we only consider the behavior of the softer theory in the symmetric phase, as that is sufficient to test the onset of non-perturbativity.

As a starting point, we consider diagrams that contain only $\bar{g}_3^2 B_i^2 \phi^\dagger \phi$ interactions. In the symmetric phase, the effective expansion parameter for this subset of diagrams is

$$\alpha_{\text{eff}} \equiv \frac{2\bar{g}_3^2}{4\pi \bar{\mu}_3} = \frac{1}{2\pi \bar{y}_c^{1/2}} \ . \tag{4.24}$$

JHEP08(2025)109

Both the soft and softer theories can only be perturbative if $\alpha_{\rm eff} < 1$. Again working at the critical temperature $T_{\rm c}$ and using $\bar{y}_{\rm c} \approx \frac{1}{18\pi^2\bar{x}}$, this yields the condition

$$\bar{x} \ll \frac{2}{9} \approx 0.22\,. \tag{4.25}$$

This constraint is equivalent to demanding that mass of the Higgs $m_h \sim \bar{\mu}_3$ is larger than the non-perturbative scale $\Lambda_{\rm NP} \equiv \frac{\bar{g}_3^2}{4\pi}$, thereby avoiding the Linde IR problem. A very similar bound can be obtained by noting that perturbation theory is expected to break down in the vicinity of the critical point at $\bar{x}_{\rm c} \approx 0.28$ due to the associated divergence of the correlation length $\xi = 1/\bar{\mu}_3$. On a quantitative level, the relevant statement is that perturbation theory is expected to break down if the Ginzburg-criterion [84]

$$\frac{1}{2}\bar{g}_3^2\varphi_{\rm min}^2 \gg \xi^{2-d}\,, \tag{4.26}$$

is violated in $d = 3$ dimensions. Again working at the critical temperature $T_{\rm c}$ and using $\varphi_{\rm min} = \frac{1}{3\pi\bar{x}}$ and $\bar{y}_{\rm c} = \frac{1}{18\pi^2\bar{x}}$, this gives the constraint

$$\bar{x} \ll \Big(\frac{1}{18\pi^2}\Big)^{1/3} \approx 0.18\,, \tag{4.27}$$

which is very similar but somewhat more stringent than eq. (4.25).

Finally, since the parameter x receives loop corrections from integrating out both the hard and soft scales, one might also be worried that sufficiently small values of x are fine-tuned. This concern is more immediate in case of the softer theory, since the matching contribution from integrating out the soft scale is larger than the hard scale contribution. Indeed, choosing the matching scale such that thermal logarithms vanish (*viz.* $L_b = 0$), one has

$$\bar{x} = x_{\rm LO} - \frac{\sqrt{3}\,g}{8\pi} + \frac{g^2}{8\pi^2} + \mathcal{O}(g^3)\,, \tag{4.28}$$

which implies that values of x much smaller than

$$\delta\bar{x}_{\rm 1loop} = \frac{\sqrt{3}}{8\pi}g \approx 0.07\,g\,, \tag{4.29}$$

require large cancellations between loop-orders, leading to fine-tuning and the associated instability of the perturbative expansion. However, since this constraint is less stringent than condition (4.22), it is fortunately not relevant in practice.

Summary. Combining the aforementioned constraints and working at the critical temperature, we find that the softer EFT remains consistent and perturbative in both the symmetric and the broken phase if

$$0.18\,g \ll \bar{x} \ll 0.18\,. \tag{4.30}$$

This narrow region suggests that the softer EFT should be applied with caution, particularly in the broken phase, where it becomes inconsistent for $\bar{x} < 0.18\,g$. In contrast, eq. (4.18) implies that in the symmetric phase, the softer EFT remains consistent for much smaller

JHEP08(2025)109

values, breaking down only at $\bar{x} < 0.017\, g^2$. Therefore, one viable approach for the description of strong first-order transitions may be to use the softer EFT only for computing the effective potential in the symmetric phase, while using complementary techniques [85, 86] for the computation in the broken phase.

The soft theory remains consistent and perturbative at the critical temperature T_c in a larger regime

$$0.051 g^2 \ll x \ll 0.18 \,. \tag{4.31}$$

For even smaller values of x, higher-dimensional operators start to contribute at leading order to the soft theory and eventually dominate the effective potential. In this regime, the high-temperature expansion breaks down, which also means that thermodynamics cannot be studied using non-perturbative lattice simulations that are performed in the EFT with only super-renormalizable operators. Any accurate study in the small-x region then necessitates a computation without resorting to high-temperature expansions; see e.g. [85, 87].

We note that our findings can readily be generalized to more general gauge groups. In particular, SU(N) theories typically exhibit larger Debye masses than the U(1) theory due to group factors (see also footnote 3), which would extend the regime of consistency for the soft and softer theories to smaller values of x. However, relatively large gauge couplings, similar to the SM SU(2) gauge coupling $g_2^2 \sim 0.4$, restrict the regime of consistency to larger values of x. Furthermore, for a SU(2) theory with a scalar in the fundamental representation, the critical endpoint is located well below that of the U(1) case. We therefore expect perturbativity to break down for smaller x values compared to the Abelian Higgs model, further limiting the regime in which perturbative techniques can be applied.

4.3 Impact of higher-dimensional operators

To investigate the impact of the $(\phi^\dagger\phi)^3$ operator on the strength of the phase transition in a more quantitative way, we consider the ratio

$$R \equiv \frac{\alpha(T_\mathrm{c})}{\alpha_{c_6=0}(T_\mathrm{c})} \,. \tag{4.32}$$

Working with the (DR-A) setup, we immediately find the analytic expression

$$R = \frac{9}{4\bar{r}}\left(\overline{\mathcal{F}}_+ - \overline{\mathcal{F}}_-\right)^2 = 1 - \frac{8\bar{r}}{27} + \mathcal{O}(\bar{r}^2) \,. \tag{4.33}$$

Finding an exact analytic expression or R in the (DR-B) setup is challenging due to the non-analytic structure of the effective potential (4.12). Instead, we determine the ratio numerically. However, an analytic estimate for R can still be obtained by approximating the effective potential with eq. (3.26), where the Debye mass m_D is set to zero. This yields the ratio

$$R \approx \frac{9}{4r}\left(\mathcal{F}_+ - \mathcal{F}_-\right)^2 = 1 - \frac{8r}{27} + \mathcal{O}(r^2) \,, \tag{4.34}$$

which we shall compare to the full numerical result in the regime where the effects of c_6 become relevant.

JHEP08(2025)109

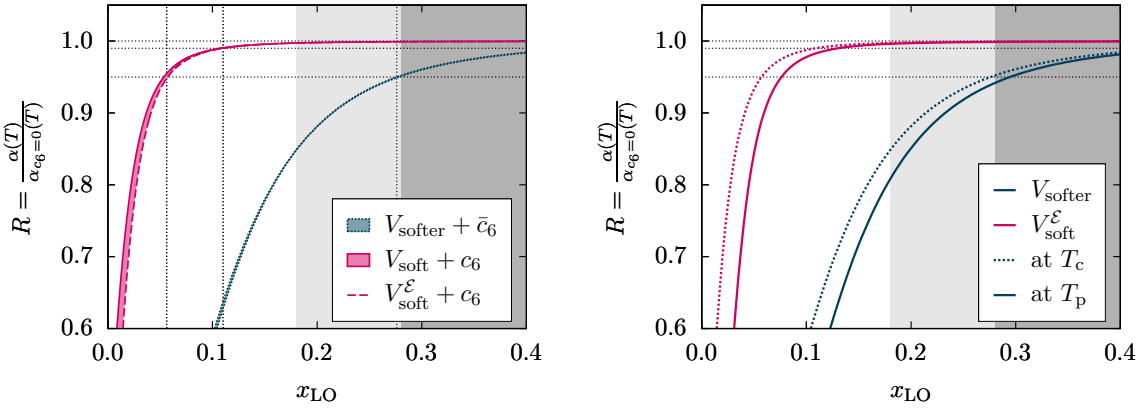

Figure 1. Impact of the $(\phi^\dagger\phi)^3$ operator on the transition strength α for $g_0 \equiv g(\bar{\Lambda} = \overline{T}) = 1$ and various $x_{\mathrm{LO}} \approx x \approx \bar{x}$. Left: blue lines are obtained from the softer-induced potential (3.25) and magenta lines from the soft-induced potential (3.24). Uncertainty bands arise from varying the hard-to-soft matching renormalization scale within $\bar{\Lambda} \in [\overline{T}, 5\overline{T}]$ where $\overline{T} \equiv 4\pi e^{-\gamma_{\mathrm{E}}} T$ and $x_{\mathrm{LO}} \equiv x_{\mathrm{LO}}(\bar{\Lambda} = \overline{T})$. The dashed magenta line depicts the $m_{\mathrm{D}} \to 0$ limit for $\bar{\Lambda} = \overline{T}$ using eq. (3.26). Horizontal dotted lines mark relative differences of 5% and 1% compared to the result without the sextic operator. The dark gray region is excluded by the critical endpoint $\bar{x}_{\mathrm{c}} \approx 0.28$ [50] and the light gray region is excluded by perturbativity constraints (4.30). The soft-scale contribution to α has a significantly greater impact than that of the hard scale alone. For the soft potential (cf. section 3.3), and strong transitions (small x), the numerical evaluation of eq. (3.24) agrees with its dashed analytical estimate (3.26). Right: the same ratio as on the left but at T_{c} (dotted) and T_{p} (solid) using $\bar{\Lambda} = \overline{T}$.

Figure 1 (right) depicts the various expressions of the ratio R as a function of the reference value $g = 1$ and $x_{\mathrm{LO}} \equiv \lambda/g^2$ at T_{c}. The blue lines are obtained in the (DR-A) setup, while the magenta lines are obtained in the (DR-B) setup. The shading indicates the region with $x_{\mathrm{LO}} > 0.2$, where our current perturbative approach is not applicable due the Linde IR problem. The softer theory is expected to be inconsistent for $\bar{x} < 0.2$ since higher-dimensional operators start to contribute to the effective potential at leading order. Indeed, figure 1 shows that the $(\phi^\dagger\phi)^3$ operators rapidly becomes dominant for smaller values of $x_{\mathrm{LO}} \approx \bar{x}$, and that correctly accounting for it significantly decreases the transition strength. For sufficiently low $\bar{x}_{\mathrm{LO}}$, the value of α becomes negative since it is dominated by $\bar{c}_6$ through eq. (4.9), which further indicates that this regime is unphysical.

On the other hand, the soft theory is expected to remain consistent for significantly smaller values of x. In the plot, the $(\phi^\dagger\phi)^3$ operator becomes dominant for $x_{\mathrm{LO}} \lesssim 0.05$. In the intermediate regime, $0.05 < x_{\mathrm{LO}} < 0.2$, where we expect the soft theory to be applicable, it decreases the strength of the transition by less than 10%. We also observe that the analytical estimate (4.34) is in excellent agreement with the full numerical result for R in the soft theory.

Overall, both the soft and softer theories become increasingly unreliable for small values of x_{LO}, where the high-temperature expansion is expected to break down. While our analysis has focused on the critical temperature, there is no reason to expect that neglecting higher-dimensional operators would yield more accurate results for e.g. α at lower temperatures, particularly below T_{c}, where bubble nucleation occurs. Indeed, we have already plotted the ratio R at the percolation temperature T_{p}, where the transition completes, as shown on the

JHEP08(2025)109

right-hand side of figure 1. In section 5, we explore how T_p is determined by estimating the statistical contribution to the bubble nucleation rate and relating it to cosmological evolution.

4.4 Comparing higher-dimensional operators and loop corrections

Given the stringent consistency and perturbativity constraints on the softer EFT, one natural question that arises is what role the higher-dimensional operators actually play in a perturbative computation of the effective potential. Our previous discussion provides a clear answer for both limiting cases of $\bar{x}$:

- For $\bar{x} > 0.2$, the softer theory is consistent but non-perturbative, which means that loop corrections dominate the effective potential, rendering a perturbative computation unfeasible, while higher-dimensional operators are essentially irrelevant.
- For $\bar{x} < 0.2\,g$, the softer theory is formally perturbative, so that loop corrections remain subdominant. However, higher-dimensional operators start contributing at leading order and ultimately lead to the breakdown of the high-temperature expansion.

But what about the intermediate regime $0.2\,g < \bar{x} < 0.2$? In the symmetric phase, spatial gauge boson modes are approximately massless, leading to a Linde problem at the ultrasoft scale. The resulting non-perturbative contributions to the effective potential are expected to scale as

$$V_\mathrm{NP} \sim \frac{\Lambda_\mathrm{NP}^3}{4\pi} = \frac{\bar{\mu}_3^3}{4\pi}\Big(\frac{1}{(4\pi)^2 y}\Big)^{\frac{3}{2}}\,, \qquad\qquad \Lambda_\mathrm{NP} = \frac{\bar{g}_3^2}{4\pi}\,. \tag{4.35}$$

In comparison, the leading contribution due to higher-dimensional operators scales as

$$V \supset \frac{\bar{\mu}_3^3}{4\pi}\Big(\frac{1}{(4\pi)^2 y}\Big)^2\Big(\frac{\bar{\mu}_3}{m_\mathrm{D}}\Big)^3\,, \tag{4.36}$$

which implies that higher-dimensional operator contributions are expected to be small compared to non-perturbative corrections, and therefore largely unimportant for the computation for the effective potential in the symmetric phase.

A priori, we expect higher-dimensional operators to be relatively more important in the broken phase, since they can contribute to the effective potential at tree level. Since we already include the leading $\frac{g_3^3\phi^3}{6\pi}$ term from one-loop gauge boson diagrams, the main question is whether the $(\phi^\dagger\phi)^3$ contribution is substantial compared to the size of the neglected higher-loop corrections. Adapting the power counting from [76], at the critical temperature T_c, and using $v \approx \frac{\bar{g}_3}{3\pi\bar{x}}$ as well as $\bar{y}_\mathrm{c} \approx \frac{1}{18\pi^2\bar{x}}$, higher-order loop corrections to the effective potential in the broken phase scale as

$$\frac{(\bar{g}_3 v)^3 x^{\frac{n_\lambda+m}{2}}}{4\pi}\Big(\frac{\bar{g}_3}{4\pi v}\Big)^{\ell-1} \approx \frac{\bar{g}_3^6}{108\pi^4}\Big(\frac{3}{4}\Big)^{\ell-1} x^{-4+\ell+\frac{n_\lambda+m}{2}}\,, \tag{4.37}$$

where ℓ denotes the loop order and n_λ the number of Higgs self-interaction vertices. The parameter $0 \leq m \leq 3$ depends on the effective mass scale of the diagram. In diagrams without Higgs self-interactions, $m = 0$ since the effective mass scale is determined by the gauge boson mass, and in pure scalar diagrams without vector boson lines, $m = 3$ since the effective

JHEP08(2025)109

mass scale is determined by the Higgs mass. Using (3.21), (4.37), and $\bar{g}_3^2 = g^2 T + \mathcal{O}(g^4)$, this implies the next-to-leading (NLO) loop correction, generated by two-loop gauge boson diagrams with $n_\lambda = m = 0$, is expected to be subdominant compared to the $(\phi^\dagger\phi)^3$ operator if

$$\bar{x} < \left(\frac{2}{\sqrt{3}\,(3\pi)^3}\right)^{\frac{1}{4}} g^{\frac{3}{4}} \approx 0.19\, g^{\frac{3}{4}} \ . \tag{4.38}$$

The analysis in [76] includes diagrams up to N^{4}LO, which scale as $x^{-1/2}$, but neglects N^{5}LO diagrams with $\ell = 2$ and $n_\lambda + m = \ell + 2$. These neglected diagrams are expected to be subdominant compared to $(\phi^\dagger\phi)^3$ contributions if

$$\bar{x} < \left(\frac{2}{3^{\frac{1}{2}}(3\pi)^3}\right)^{\frac{1}{6}} g^{\frac{1}{2}} \approx 0.33\, g^{\frac{1}{2}} \ . \tag{4.39}$$

These estimates show that for small x, uncertainties from neglecting higher-dimensional operators outweigh those from neglecting higher-loop corrections. Specifically, for $\bar{x} < 0.19\, g^{\frac{3}{4}}$, the contributions due to higher-dimensional operators dominate even over the leading two-loop contributions to the effective potential.

5 Gravitational wave prospects

In the previous section, we discussed the impact of higher-dimensional operators on the phase transition strength at the critical temperature. To relate these findings to gravitational wave predictions, we need to consider the impact below the critical temperature, and in particular at the percolation temperature T_p, where the phase transition is completed.

To analyze the leading effect of the sextic operator, we consider the leading-order potentials of eqs. (3.31a) and (3.31c) and use `FindBounce` [88] to construct a semi-classical bounce solution v_b that extremizes the effective action

$$S_3[v] \equiv \int_{\mathbf{x}} \left[\frac{1}{2}(\partial_i v)^2 + \widetilde{V}(v)\right], \qquad \widetilde{V}(v) \equiv \frac{y}{2}v^2 + \frac{x}{4}v^4 + \frac{c_6}{8}v^6 - \frac{1}{6\pi}v^3\,, \tag{5.1}$$

and thus solves the classical equation of motion $\delta S_3[v_b] = 0$. This stationary solution corresponds to the physical profile of the critical bubble, and the resulting extremal value of the effective action $S_3[v] = S_3(x, y, c_6)$ is the main ingredient needed to determine the thermal bubble nucleation rate at leading order in the semi-classical approximation or nucleation EFT [62]. This formulation guarantees theoretical self-consistency, including the gauge-invariance [70, 89], and avoids double counting contributions of different energy scales [62]. In particular, it would allow for a consistent inclusion of all large thermal corrections from the hard scale, including two-loop thermal masses essential for the renormalization scale independence [24, 90]. We emphasize that resolving these aforementioned issues is essential for theoretical consistency and ensuring physically meaningful results, but commonly not achieved, cf. e.g. [91–94].

The form of the potential in (5.1) encompasses both the softer-induced potential (3.31a) and the approximated soft-induced potential (3.31c). Higher-dimensional kinetic (or derivative) effects from the scalar and vector sectors of the corresponding EFT also contribute to

JHEP08(2025)109

the effective action. These effects can arise both from a derivative expansion of the prefactor A in the nucleation rate and from the high-temperature expansion. Since the derivative expansion does not necessarily converge at the tail of the bounce [25, 71], we do not include its higher-order derivative terms explicitly in eq. (5.1). Instead, we argue that their effects can be more systematically included through the corresponding fluctuation determinants [71, 95, 96].

Using the same approach as [24, 76, 97] (also cf. [98]), we follow [99] and define the percolation time $t_{\rm p}$ as the time at which volume fraction of space in the metastable phase is $f(t_{\rm p}) = 1/e$. While it should be possible, in principle, to capture the time-evolution and higher-orders of this volume fraction from first principles using perturbative real-time computations [100–102] or non-perturbative, numerical simulations [103–107], the standard approach in the literature is to follow [108, 109] and utilize the phenomenological expression

$$f(t) = e^{-I(t)}\,, \qquad I(t) \equiv \int_{t_{\rm c}}^{t} {\rm d}t'\,\Gamma(T(t'))V(t,t')\,, \qquad V(t,t') = \frac{4\pi}{3}v_w^3(t-t')^3\,. \tag{5.2}$$

Here, $t_{\rm c}$ is the time at which the temperature of the early universe plasma is equal to the critical temperature $T_{\rm c}$, $\Gamma(t) = A(t)\,e^{-S_3(t)}$ the bubble nucleation rate (i.e. the probability of nucleation per unit time per unit volume), $V(t,t')$ the volume of a (spherically symmetric) bubble that nucleated at t' at some later time t, v_w the terminal bubble wall velocity, and the exponentiation in eq. (5.2) accounts for the fact that bubbles can overlap. Formula (5.2) implicitly assumes the thin-wall approximation, where the volume occupied by the bubble walls is negligible, and that all bubbles grow at the same rate.

The explicit expression for $V(t,t')$ in terms of $v_w(t)$ also assumes that the bubble wall velocity rapidly reaches its terminal value, and that this value remains approximately constant over time. Further assuming that the non-equilibrium prefactor $A(t)$ is approximately constant, the volume fraction integral becomes

$$I(t_{\rm p}) \approx \frac{4\pi v_w^3}{3} A \int_{t_{\rm c}}^{t_{\rm p}} {\rm d}t' e^{-S_3(t')}(t_{\rm p}-t')^3 \approx 8\pi v_w^3 \frac{A\,e^{-S_3(t_{\rm p})}}{\beta^4} \begin{cases} 1 & \gamma \ll 1 \\ \gamma^3 e^{\gamma} & \gamma \gg 1 \end{cases}\,, \tag{5.3}$$

where

$$\beta \equiv -\frac{{\rm d}S_3}{{\rm d}t_{\rm p}}\,, \qquad\qquad \gamma \equiv \beta(t_{\rm p}-t_{\rm c})\,. \tag{5.4}$$

The quantity β defines the inverse duration of the phase transition. The integral in eq. (5.3) has been evaluated by expanding the action to linear order in $t'-t_{\rm p}$,

$$S_3(t) = S_3(t_{\rm p}) + \frac{{\rm d}S_3}{{\rm d}t_{\rm p}}(t-t_{\rm p}) + \mathcal{O}\left((t-t_{\rm p})^2\right)\,. \tag{5.5}$$

This approximation captures the correct leading-order dynamics of bubble nucleation because the integrand in eq. (5.3) is exponentially suppressed and therefore rapidly decreases for smaller values of t'. This also further justifies our assumption that both A and v_w can be treated as approximately constant. Nevertheless, higher-order corrections can be systematically included by evaluating eq. (5.3) numerically, while tracking the full temperature dependence of each quantity [103, 105, 106].

JHEP08(2025)109

Using the approximate expression on the right-hand side of eq. (5.3) and assuming that $\gamma \ll 1$, the percolation condition $I(T_\mathrm{p}) = 1$ for maximally colliding bubbles[5] thus yields the relation

$$S_3(T_\mathrm{p}) = \ln(8\pi) + 3\ln v_w + \ln\frac{A}{H^4} - 4\ln\frac{\beta}{H}\,. \tag{5.6}$$

In a radiation-dominated FRW cosmology with an ideal gas equation of state, the Hubble rate is given by[6]

$$H(T) = \sqrt{\frac{4g_\star\pi^3}{45}}\frac{T^2}{M_\mathrm{Pl}}\,, \qquad\qquad M_\mathrm{Pl} = 1.22\times 10^{19}\ \mathrm{GeV}\ . \tag{5.7}$$

At this stage, we have not yet specified explicit expressions for the prefactor A or the bubble wall velocity v_w. However, since these quantities appear in eq. (5.6) only logarithmically, their exact values are unimportant at leading order; it suffices to estimate their order of magnitude. Accordingly, we approximate $A \approx T^4$ by dimensional analysis and take $v_w \sim 1$, and then impose the approximate condition [71, 76, 97, 111]

$$S_3[v_b]|_{T=T_\mathrm{p}} \approx 126\,, \tag{5.8}$$

to find the percolation temperature. Inverting this condition, one obtains a relationship $y(T_\mathrm{p}) = y_\mathrm{p}(x, c_6)$ that makes it possible to find the percolation temperature T_p purely in terms of the 3d quantities y, x, c_6, allowing for efficient scans in the (x, y)-plane (while also varying c_6). However, it is also straightforward to relax the assumptions underlying eq. (5.8) for a given parameter point of the parent theory, and to determine T_p directly from eq. (5.6). For vanishing c_6, one could find a fit function for $S_3(x, y, c_6 = 0)$ in analogy to the one in [97].

For non-zero c_6, deriving a general fit becomes more challenging. Instead, we evaluate S_3 using eq. (5.1), including the soft enhancement with the coefficient $c_6 = c_6(g)$ at fixed g. This approach allows us to illustrate our key findings during the parameter scan outlined below. The corresponding fit takes the form

$$S_3 = \kappa\left[A + B\gamma + \frac{C}{1-\gamma} + \frac{D}{(1-\gamma)^2}\right], \tag{5.9}$$

where $\kappa = 64\pi^2 y^{3/2}$, $\gamma = y/y_\mathrm{c}(x, c_6)$ with $y_\mathrm{c}(x, c_6)$ given in eq. (4.15). In the soft theory, the action fitting parameters are given in table 1 (left) while in the softer theory, they depend on the value of g as given in table 1 (right). In the softer theory, the fit is also more sensitive to values of g as the fitted $S_3(x, y, \bar{c}_6)$ utilizes $\bar{c}_6 \sim g^3$ from eq. (3.21) instead of $c_6 \sim g^6$ from eq. (3.10).

The right panel in figure 1 compares the ratio of the transition strength $R = \alpha(T)/\alpha_{c_6=0}(T)$ at the critical temperature (dotted lines) and the percolation temperature (solid lines). As

[5]The percolation condition used here is more conservative than the standard one [94, 110], which requires the probability of a point in space remaining in the false vacuum to be $P(T_\mathrm{p}) = e^{-I(T_\mathrm{p})} \simeq 71\%$ corresponding to $I(T_\mathrm{p}) \approx 0.34$.

[6]The effective number of radiation degrees of freedom, $g_\star$, explicitly enters this relation. If our setup is treated as a dark sector decoupled from the SM, the numerical values of eq. (5.7) differ from those in the SM, as discussed below eq. (4.2).

JHEP08(2025)109

A	B	C	D
0.751	-0.413	0.704	0.075

g	A	B	C	D
0.9	-30.418	56.244	-2.310	0.267
0.7	3.353	-2.030	0.484	0.206
0.5	4.178	-4.383	0.945	0.196

Table 1. Soft (left) and softer (right) theory fit parameters for the 3d action (5.9).

expected, for each fixed $x_{\rm LO}$ the sextic operator is slightly more important at $T_{\rm p} < T_{\rm c}$, and reduces the transition strength by $\mathcal{O}(1\%)$ more than at the critical temperature in the regime that is still within reach of the high-temperature expansion. For the inverse duration, we find a smaller $\sim 1-4\%$ reduction due to the sextic operator in the range $x \in [0.02, 0.1]$, concluding that this quantity appears less sensitive compared to α, based on our simple leading-order estimates.

Besides the transition strength α, gravitational wave predictions also depend on average bubble separation $R_* H_*$ (relative to the Hubble parameter in radiation dominated epoch), which can be related in our setup to the inverse duration of the transition β, via [112] (cf. [99])

$$R_* H_* \approx (8\pi)^{\frac{1}{3}} \max\{v_w, c_s\} \Big(\frac{\beta}{H_*}\Big)^{-1} , \tag{5.10}$$

where for the strong transitions in our case $v_w > c_s$. We compute the inverse duration of the transition by using the relation [17]

$$\frac{\beta}{H} = T \frac{\mathrm{d}S_3[v_b]}{\mathrm{d}T} \approx \eta_y \partial_y S_3[v_b]\Big|_{T=T_{\rm p}} . \tag{5.11}$$

To connect our computation to observational prospects of LISA and DECIGO detectors, we scan over the model parameters of the parent theory, and compute thermal parameters α and β/H at $T_{\rm p}$.

First, we work in the softer EFT (DR-A). To employ eqs. (4.7) and (5.11), we insert the leading-order temperature dependence of y via its η-function

$$\eta_y \equiv T \frac{\mathrm{d}y}{\mathrm{d}T} \approx -\frac{2}{g^4} \frac{\mu^2}{T^2} = \frac{1}{g^4} \frac{M^2}{T^2} , \tag{5.12}$$

where we have used leading-order matching relations, as well as tree-level relation $\mu^2 = -\frac{1}{2} M^2$ between the 4d scalar mass parameter and physical scalar mass M.[7] Next, we could directly compute thermal parameters $T_{\rm p}$, α and β/H in terms of three input parameters g, $\lambda = x_{\rm LO} g^2$ (using the LO relation) and M. However, we can simplify the parameter scan considerably by eliminating the ratio M/T. To this end, we note that at the critical temperature $y(T_{\rm c}) = y_{\rm c}(x) = 1/(18\pi^2 x)$ and by using the leading-order matching relation, we find

$$\frac{M^2}{T_{\rm c}^2} \approx \frac{g^2}{2} - \frac{g^4}{9\pi^2 x_{\rm LO}} + \frac{2 g^2 x_{\rm LO}}{3} - \tau \frac{g^3}{2\sqrt{3}\pi} \equiv F(g, x_{\rm LO}, \tau) \approx \frac{M^2}{T_{\rm p}^2} . \tag{5.13}$$

[7] To relate the scalar mass parameter to its pole mass M at higher orders as well as relating other $\overline{\rm MS}$ and physical parameters, one needs to employ zero-temperature one-loop vacuum renormalization, cf. e.g. [7, 18].

JHEP08(2025)109

For convenience, we defined an auxiliary parameter $\tau = 1$ for the softer theory, while for the soft enhancement $\tau = 0$. We know that for a radiatively generated barrier, the amount of supercooling, i.e. the difference $\Delta T \equiv T_c - T_p$, is small [76]. Therefore, we also approximate $M^2/T_p^2 \approx F(g,x)$ using eq. (5.13). We have thus eliminated the ratio M^2/T_p^2 in terms of g and x, and can hence express

$$\frac{\beta}{H} \approx \frac{1}{g^4} F(g,x,1)\partial_y S_3(y_p,x,c_6)\,, \tag{5.14}$$

$$\alpha \approx \frac{30}{(2\pi)^2 g_\star} g^2 F(g,x,1)\partial_y \Delta\widetilde{V}_{\text{softer}}(y_p,x,c_6)\,, \tag{5.15}$$

at leading order. Within these approximations, we can readily scan the entire parameter space, i.e. the (x,g)-plane. For this, we perform a uniform scan with

$$\begin{aligned} x &\in [0.01, 0.3] && \text{with step size} && \Delta x = 0.002\,, \\ g &\in [0.1, 0.9] && \text{with step size} && \Delta g = 0.02\,, \end{aligned} \tag{5.16}$$

and recast our result in the $(\alpha_p, \beta/H_p)$-plane in figure 2 (top row).

Before discussing the result, we note that our discussion so far has considered only the softer EFT (DR-A). Since we have already concluded that the soft-to-softer EFT construction is unreliable for strong transitions (at small x), we also consider the soft-to-supersoft EFT utilizing the approximated soft-induced effective potential (3.26). In this case, the formulae for α and β/H need to be adjusted to include the effects of soft enhancement factor $\mathcal{E} = \frac{3}{2}$. This yields

$$\frac{\beta_\mathcal{E}}{H} \approx \frac{\mathcal{E}^{-\frac{4}{3}}}{g^4} F(g,x,0)\,\partial_Y S_3(Y_p,X,c_6)\,, \tag{5.17}$$

$$\alpha_\mathcal{E} \approx \frac{30}{(2\pi)^2 g_\star} \mathcal{E}^{\frac{2}{3}} g^2 F(g,x,0)\,\partial_y \Delta\widetilde{V}_{m_D^2 \ll h_3 v^2}(y_p,x,c_6)\,, \tag{5.18}$$

where we defined the notation $X \equiv \mathcal{E}^{-\frac{2}{3}} x$ and $Y \equiv \mathcal{E}^{-\frac{4}{3}} y$. The subscript $\{\alpha,\beta\}_\mathcal{E}$ indicates the inclusion of the soft enhancement.

Figure 2 depicts the predicted values of α and β for various values of g and x. The top row is obtained using the soft-to-softer EFT setup (DR-A), while the bottom row is obtained using the soft-to-supersoft EFT (DR-B). In each plot, the value of x decreases from left to right, with the smallest x values mapping into the bottom right corner. The points approach the tentative LISA sensitivity window[8] for large values of α and small values of β/H.[9] To showcase the dependence on g, the plots of the left-hand side display results for three fixed values of $g = 0.5, 0.7, 0.9$ while varying x. In each case, including the leading effect of the dimension-six operator reduces α. The branching between the curves with and without higher-operator effect increases as α and β approach the LISA sensitivity region, which

[8] The sensitivity regions are taken purely tentative at a wall velocity $v_w = 0.95$ for LISA at SNR = 5 [114] with $\mathcal{T} = 4$ year mission duration [112] and DECIGO with the *Correlation* design [113] were taken from [115]. As discussed below eq. (4.2), $g_\star = 4$ which differs from the SM one used in the sensitivity regions.

[9] For a signal to be visible for LISA and DECIGO, the temperature T_p has to be in a $\sim 100\,\text{GeV}$ range to produce a GW power spectrum in the appropriate frequency range. To ensure this, we have implicitly assumed here that the scalar mass M is $\mathcal{O}(100\text{ GeV})$.

JHEP08(2025)109

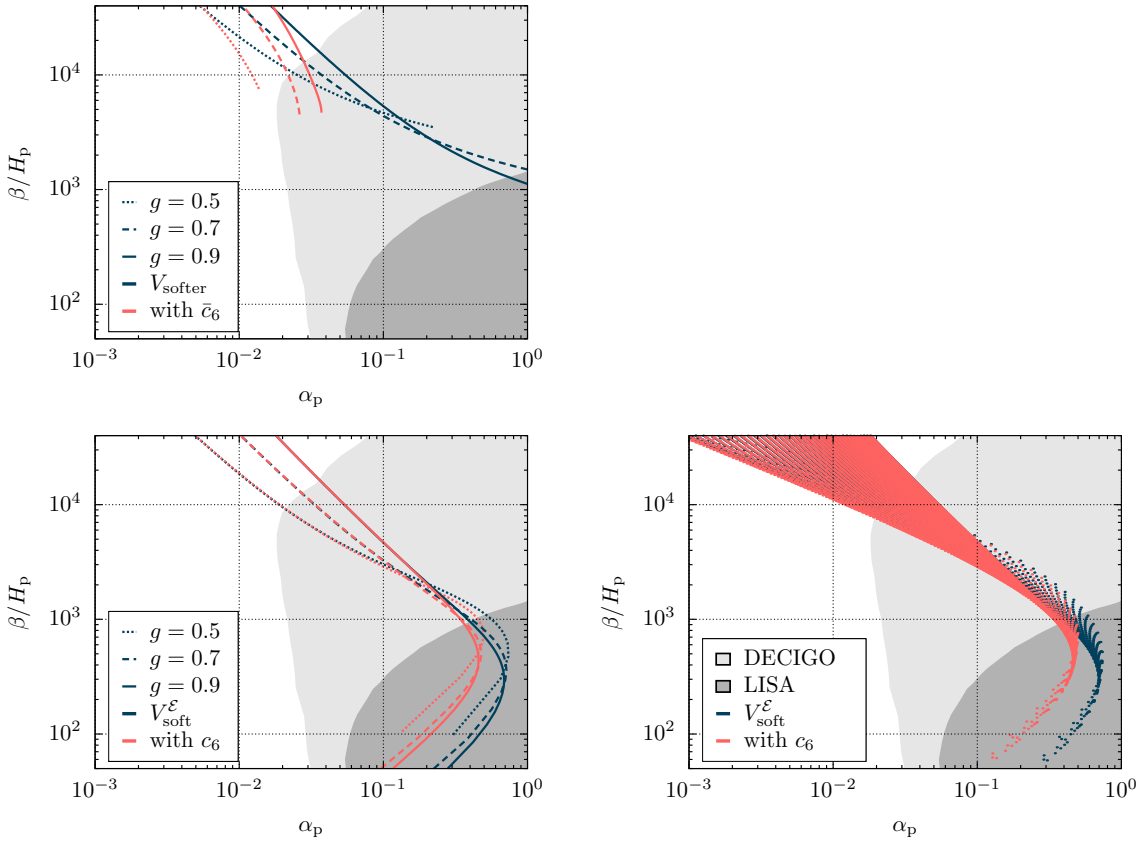

Figure 2. Top left: parameter scan over x of the softer EFT potential (3.25) at fixed values $g = 0.5$ (dotted), $g = 0.7$ (dashed), and $g = 0.9$ (solid), were x decreases from left to right. Bottom row: as the top row but for the soft EFT potential (3.24) which exhibits soft enhancement due to the included temporal mode. Bottom right: parameter scan using the grid (5.16) in the $(\alpha_\mathrm{p}, \beta/H_\mathrm{p})$-plane with (red) and without (blue) LO effect from c_6. Also shown are the tentative sensitivity regions for LISA [112] and DECIGO [113]; see footnote 8.

indicates the increasing uncertainty and an eventual breakdown of the high-temperature expansion. The same trend is evident in the plot on the bottom right-hand side of figure 2, where the tail containing the strongest and longest transitions shifts to lower values of α.

Comparing the top and bottom plots on the left-hand side, we observe that it is crucially important to treat the temporal mode correctly for strong transitions. In the top row, including sextic operator effects shifts all points within the reach of LISA and DECIGO toward undetectably small values of α. This signals the limitation of the softer EFT at small x, and is consistent with the behavior in figure 1. Numerically, in the regime of even larger x, the curves for the softer EFT with $\bar{c}_6 \neq 0$ and $c_6 = 0$ do not fully converge. This is due to the limitations of our simplified scanning setup, described by the fit in eq. (5.9), which is more sensitive in this region to large derivatives of $\frac{\mathrm{d}}{\mathrm{d}\ln T} S_3(x, y, \bar{c}_6)$. While this regime lies outside the focus of our analysis, a more accurate approach would be a direct computation of the bounce action.

The bottom row of figure 2 shows that the temporal mode strengthens the transition in the small-x regime due to soft enhancement, shifting points toward larger α. However, even

JHEP08(2025)109

with this improved treatment of the temporal mode, the impact of the sextic operator remains significant in the tentative LISA window and is still non-negligible within the tentative sensitivity range of DECIGO. This suggests that even if the temporal modes are treated correctly, the high-temperature expansion may become unreliable for sufficiently strong transitions such as those targeted by next-generation GW detectors.

In this regard, our work builds on and extends the findings of [17], which concluded that, in the absence of higher-dimensional operators, radiatively-generated one-step transitions strong enough to be detectable by LISA cannot be reliably described. Our results suggest an even stronger conclusion. The high-temperature expansion itself may break down entirely, thereby invalidating the EFT description. While we arrive at this result within a simplified toy model, we expect the conclusion to hold more broadly. This is due to the generic infrared structure of gauge-Higgs theories and the qualitatively similar features of dimensional reduction, including the emergence of sizable higher-dimensional operators in the regime of strongest transitions. To reach these conclusions regarding the relevance of higher-dimensional operators, we adopted the following simplifying assumptions: (i) leading-order in dimensional reduction, (ii) leading-order in the nucleation effective theory, and (iii) negligible supercooling, as noted below eq. (5.13). Each of these approximations is individually robust when including higher-order corrections. Accordingly, we anticipate that our main conclusions will remain valid when such corrections are taken into account.

6 Conclusions and outlook

Comprehensively understanding the effects of higher-dimensional operators in thermal EFTs for the electroweak phase transition has been a long-standing challenge. In this article, we take a significant step toward this goal by studying the Abelian Higgs model as a simplified toy model. This model shares many important features with more complex and realistic gauge-Higgs theories relevant for electroweak phase transitions, allowing us to probe the impact of higher-dimensional operators in a controlled setting.

In particular, we have achieved a complete matching of the marginal sextic operators by constructing a complete, minimal, and fully gauge-invariant operator basis in both the soft and softer EFTs. This step is crucial for ensuring the theoretical consistency of the EFT framework and accurately capturing the physical properties of the full theory. As is often the case in advancing the understanding of hot electroweak-like theories, we have drawn inspiration from analogies in hot QCD [11, 13] and weaponized existing tools for general EFT matching, such as `Matchete` [116]. We anticipate that these developments will enhance the capabilities of `DRalgo`[73], which, in turn, utilizes functionalities from `GroupMath` [117].

We have also clarified the role of temporal gauge boson modes by demonstrating that treating them within the framework of soft-to-softer EFT matching — i.e., integrating out temporal modes and absorbing their effects into the scalar sector parameters [7, 69] — induces large contributions from marginal operators in the regime of strong transitions. As a result, soft-to-softer EFT matching proves unreliable for strong transitions.[10] Instead,

[10]This conclusion is softened in theories with larger Debye masses, such as SU(N) theories with many charged fermions, where the softer EFT is expected to perform better. This could be tested by repeating a similar study within SU(2) gauge-Higgs theory and by computing higher-loop corrections akin to [76], while

JHEP08(2025)109

temporal modes should be treated within the framework of soft-to-supersoft matching [64], as implemented in [25, 71, 72, 121]. This refinement leads to an enhanced potential barrier compared to including only spatial mode contributions.

For radiatively induced phase transitions in the Abelian Higgs model, we demonstrated that including the leading effect of the sextic $(\phi^\dagger\phi)^3$-operator in the effective potential leads to a significant $\mathcal{O}(5\%)$ reduction in the phase transition strength in the regime of strong transitions that are still within reach of the high-temperature expansion. For even stronger transitions, the sextic operator contribution quickly increases. This signals a potential breakdown of the EFT description due to a lack of thermal scale hierarchies, as the large background field value induces masses for the Matsubara zero-modes that are comparable to the hard scale. Such a breakdown would not only limit the applicability of state-of-the-art perturbative techniques, but also of non-perturbative lattice studies. Overcoming these limitations would require the development of new techniques to compute the phase transition thermodynamics entirely without using high-temperature expansions [85, 87], while still being able to resum infrared-sensitive contributions at small field values. Our findings highlight the importance of such endeavors, and in particular the need for direct lattice simulations of the full theory in four dimensions [4, 34, 122–124].

Extending the present study to more complicated BSM theories could help to comprehensively investigate the reliability of current state-of-the-art non-perturbative studies, such as [16, 19, 125], which rely on the high-temperature expansion and thermal EFTs that are truncated to not include marginal operators. Scrutinizing the accuracy and the limits of such analyses is of key importance to reliably predict the thermodynamics of cosmological phase transitions, which, in turn, affect open problems such as the matter-antimatter asymmetry of the universe in the framework of electroweak baryogenesis [126], as well as predictions for a gravitational wave background generated by such transitions [6, 112, 127].

For gravitational wave predictions, we found that including the sextic operator in the small-x regime decreases both α and β/H. While the reduction in β/H improves sensitivity for LISA, the overall weakening of the transition is generally unfavorable for observational prospects, which benefit from stronger phase transitions. We have found that it is indeed the strongest transitions that are most affected by higher-order operators and the associated possibility of a breakdown of the high-temperature expansion. While this puts serious limitations on the predictability of primordial remnants from thermal phase transitions at LISA and similar experiments, it also poses an opportunity to refine theoretical approaches.

Acknowledgments

We generously thank Andreas Ekstedt, Lauri Niemi and Juuso Österman for their contributions and insights at the early stages of this work. In addition, we thank Jaakko Annala, Oliver Gould, Joonas Hirvonen, Pablo Navarrete, Risto Paatelainen, Kari Rummukainen, Riikka Seppä, Kaapo Seppänen, and Jorinde van de Vis for illuminating discussions. FB and PS were supported by the Swiss National Science Foundation (SNSF) under grant PZ00P2-215997.

treating temporal gauge fields on equal footing with spatial ones. In addition, a direct comparison would require lattice studies that explicitly incorporate dynamical temporal gauge fields, cf. [74, 75, 111, 118–120].

JHEP08(2025)109

PK was supported by the SNF under grant P500PT-217885. TT was supported by the European Union (ERC, CoCoS, 101142449).

A Field redefinitions

To construct an effective field theory, one has to specify a power counting in terms of some small parameter ϵ such that, at any given order in ϵ, only a finite number of operators contribute to its action

$$S_{\text{EFT}}\left[\{\Phi_i\}\right] = \sum_{n=0}^{\infty} \epsilon^n S_n\left[\{\Phi_i\}\right] , \tag{A.1}$$

where $\{\Phi_i\}$ collectively denotes the various fields of the theory. If the action contains a term

$$S_{\text{EFT}}\left[\{\Phi_i\}\right] \supset \epsilon^n \int \mathrm{d}^d x \, \frac{\delta S_0}{\delta \Phi_i(x)} \mathcal{O}[\{\Phi_i\}](x) , \qquad n \geq 1 , \tag{A.2}$$

where $\mathcal{O}[\{\Phi_i\}](x)$ is a composite operator that depends only on fields evaluated at coordinate x, this term can be removed from the action up to corrections of order ϵ^{n+1} by means of the field redefinition

$$\Phi_i \to \widetilde{\Phi}_i - \epsilon^n \mathcal{O}[\{\widetilde{\Phi}_i\}] . \tag{A.3}$$

Since the action (A.1) must already contain all operators that are consistent with the symmetries of the effective theory, the net effect of (A.3) is to rescale the Wilson coefficients of higher-order operators.[11] Furthermore, working in dimensional regularization and excepting fermions that are subject to a chiral anomaly, it can be shown [128][12] that field redefinitions of the form (A.3) do not alter the path integral measure $\mathcal{D}\{\Phi_i\}$ in the generating functional

$$Z[J_i] = e^{iW[J_i]} = \frac{1}{\mathcal{N}} \int \mathcal{D}\{\Phi_i\} \, e^{-S_{\text{EFT}}[\{\Phi_i\}] + \int \mathrm{d}^d x J_i(x) \Phi_i(x)} , \tag{A.4}$$

which is normalized such that $Z[0] = 1$. The source term $J_i(x)\Phi_i(x)$, and with it $Z[J_i]$ as a whole, is *not* in general invariant under (A.3), but this can be shown to not affect on-shell S-matrix elements [128, 129]. We focus on the Euclidean 1PI effective action $\Gamma[\phi_i]$, which obeys the recursive relation

$$e^{-\Gamma[\phi_i]} = \int \mathcal{D}\{\Phi_i\} \, e^{-S_{\text{EFT}}[\{\Phi_i\}] + \int \mathrm{d}^d x J_i(x)(\Phi_i(x) - \phi_i)} , \qquad J_i(x) = \frac{\delta \Gamma}{\delta \phi_i(x)} . \tag{A.5}$$

For field configurations that obey the equations of motion $J_i(x) = 0$, this relation, together with the invariance of the path integral measure, implies that the effective action is not affected by the field redefinition (A.3). Since the effective potential $V(\phi)$ is just the effective

[11] Note that if Φ_i is a gauge field, the gauge-fixing and ghost Lagrangians should be considered a part of the zeroth-order effective action S_0, so that the field redefinition (A.3) implicitly changes the gauge-fixing. The original gauge-fixing can then be restored by using a normal gauge transformation.

[12] While [128, 129] only consider theories in Minkowski space, our primary focus is on Euclidean theories. However, the proof does not rely on any information about the signature of the metric tensor and hence translates to Euclidean geometry without modification.

JHEP08(2025)109

action of a constant field configuration divided by the volume of spacetime, this result implies that both the location of the minima of the effective potential as well as the value of the potential at those minima are likewise unaffected by the field redefinition.

To utilize the field redefinition (A.3) in practice, one has to identify the leading-order non-vanishing contribution to the effective action $S_{\rm EFT}$. In our setup, the first non-vanishing contributions are of $\mathcal{O}(g^2)$, so that the corresponding effective Lagrangian is

$$\mathcal{L} = D_i\phi^\dagger D_i\phi + \mu_3^2\phi^\dagger\phi + \lambda_3(\phi^\dagger\phi)^2 + \frac{1}{4}F_{ij}F_{ij} + \frac{1}{2}(\partial_i B_0)^2 + g_3^2\phi^\dagger\phi B_0^2 + \frac{1}{2}m_{\rm D}^2 B_0^2 \,. \tag{A.6}$$

This yields the equations of motion

$$D^2\phi = \left(\mu_3^2 + 2\lambda_3(\phi^\dagger\phi) + g_3^2 B_0^2\right)\phi\,, \qquad \partial^2 B_0 = \left(m_{\rm D}^2 + 2g_3^2(\phi^\dagger\phi)\right)B_0\,, \tag{A.7a}$$

$$D^2\phi^\dagger = \left(\mu_3^2 + 2\lambda_3(\phi^\dagger\phi) + g_3^2 B_0^2\right)\phi^\dagger\,, \qquad \partial_i F_{ij} = ig_3\,\phi^\dagger D_j\phi + h.c.\,, \tag{A.7b}$$

which we can use to eliminate any higher-order operator containing the terms $D^2\phi$, $D^2\phi^\dagger$, $\partial^2 B_0$, and $\partial_i F_{ij}$.

B Details of dimensional reduction

This appendix collects renormalization group equations (RGE), the matching relations of the fundamental, four-dimensional theory, defined in eq. (2.1) to its dimensionally reduced, three-dimensional, effective theory in eq. (3.4), and the thermal effective potential computed within the EFT.

B.1 Renormalization and β-functions at zero temperature

The renormalization group equations listed below are associated with the parameters of the model in eq. (2.1) and encode their running with respect to the $\overline{\rm MS}$ renormalization scale $\bar{\Lambda}$ via the β-functions. To this end, we use

$$t \equiv \ln\bar{\Lambda}^2\,, \tag{B.1}$$

where $\bar{\Lambda}^2 \equiv 4\pi e^{-\gamma_{\rm E}}\Lambda^2$, and find at one-loop level

$$\partial_t g^2 = \frac{1}{(4\pi)^2}\left(\frac{1}{3}g^4\right)\,, \tag{B.2}$$

$$\partial_t \mu^2 = \frac{1}{(4\pi)^2}\mu^2\left(4\lambda - 3g^2\right)\,, \tag{B.3}$$

$$\partial_t \lambda = \frac{1}{(4\pi)^2}\left(10\lambda^2 - 6g^2\lambda + 3g^4\right)\,. \tag{B.4}$$

B.2 One-loop dimension-six coefficients of the soft 3d EFT

Dimension-four vertices and matching relations for the Abelian Higgs model are known [69, 70]. Below we collect the results for the corresponding matching relations up to dimension-six operators and before field redefinitions. Results are given in dimensional regularization and with dimension $d = 3 - 2\epsilon$.

JHEP08(2025)109

dimension 2	
B_0^2	$Z_{B_0}\,\widehat{m}_{\rm D}^2/2$
$\phi^\dagger\phi$	$Z_\phi\,\hat{\mu}_3^2$

dimension 4	
$(\partial_i B_0)^2/2$	Z_{B_0}
$F_{ij}F_{ij}/4$	Z_{B_i}
$(D_i\phi)^\dagger(D_i\phi)$	Z_ϕ
$(\phi^\dagger\phi)^2$	$Z_\phi^2\widehat{\alpha}_{\phi^4}$
$(\phi^\dagger\phi)B_0^2$	$Z_\phi Z_{B_0}\widehat{\alpha}_{\phi^2 B_0^2}$
B_0^4	$Z_{B_0}^2\widehat{\alpha}_{B_0^4}$

Table 2. Super-renormalizable operators and their corresponding Wilson coefficients in the soft-scale 3d effective theory. Note that the wave-function renormalization constants Z_ϕ, Z_{B_0} and Z_{B_i} are subsequently reabsorbed into field operators ϕ, B_0, and B_i to ensure canonical normalization.

dimension-six operator basis	
$F_{ij}F_{ij}B_0^2$	$Z_{B_0}Z_{B_i}\widehat{\alpha}_{B_0^2F^2}$
$F_{ij}F_{ij}\phi^\dagger\phi$	$Z_{B_i}Z_\phi\widehat{\alpha}_{\phi^2F^2}$
$(D_i\phi^\dagger D_i\phi)(\phi^\dagger\phi)$	$Z_\phi^2\widehat{\alpha}_{D^2\phi^4,1}$
$(D_i\phi^\dagger D_i\phi)B_0^2$	$Z_\phi Z_{B_0}\widehat{\alpha}_{D^2\phi^2B_0^2,3}$
B_0^6	$Z_{B_0}^3\widehat{\alpha}_{B_0^6}$
$B_0^4(\phi^\dagger\phi)$	$Z_\phi Z_{B_0}^2\widehat{\alpha}_{\phi^2B_0^4}$
$B_0^2(\phi^\dagger\phi)^2$	$Z_\phi^2Z_{B_0}\widehat{\alpha}_{\phi^4B_0^2}$
$(\phi^\dagger\phi)^3$	$Z_\phi^3\widehat{\alpha}_{\phi^6}$

Redundant operators	
$(\partial_i F_{ij})^2$	$Z_{B_i}\widehat{\alpha}_{D^2F^2}$
$B_0\Box^2B_0$	$Z_{B_0}\widehat{\alpha}_{D^4B_0^2}$
$B_0^3\Box B_0$	$Z_{B_0}^2\widehat{\alpha}_{D^2B_0^4}$
$(D^2\phi^\dagger)(D^2\phi)$	$Z_\phi\widehat{\alpha}_{D^4\phi^2}$
$(\phi^\dagger\phi)(\phi^\dagger D^2\phi+h.c.)$	$Z_\phi^2\widehat{\alpha}_{D^2\phi^4,2}$
$(\partial_i F_{ij})i\phi^\dagger(D_j\phi)$	$Z_\phi Z_{B_i}^{1/2}\widehat{\alpha}_{D^2\phi^2F}$
$(\phi^\dagger\phi)B_0\Box B_0$	$Z_\phi Z_{B_0}\widehat{\alpha}_{D^2\phi^2B_0^2,1}$
$\phi^\dagger(D_i^2\phi)B_0^2+h.c.$	$Z_\phi Z_{B_0}\widehat{\alpha}_{D^2\phi^2B_0^2,2}$

Table 3. All possible dimension-six operators in the soft-scale 3d effective theory. The operators of all the redundant operators can be eliminated using the leading-order equations of motion (A.7). In the final Lagrangian, we also combine partial integration with the equations of motion to remove the operator $(D_i\phi^\dagger D_i\phi)B_0^2$ in favor of $(\phi^\dagger\phi)(\partial_iB_0\partial_iB_0)$.

In tables 2 and 3, all the operators up to dimension 6 along with their respective Wilson coefficients are listed ($D_i\equiv\partial_i-ig_3Z_{B_i}^{1/2}B_i$). Operators containing an odd number of B_0 fields are excluded because the matching conditions require them to vanish due to the Abelian nature of the theory and charge conjugation symmetry [120].

Below, we present the result of the one-loop matching between the two theories. The fundamental theory lives in $D=d+1$ spacetime and the EFT in $d=3$ spatial dimensions. Together with the field normalizations

$$Z_{B_i} = 1+\frac{1}{3}g^2\mathcal{I}_2\,, \tag{B.5}$$

$$Z_{B_0} = 1+\frac{1}{3}(4-d)g^2\mathcal{I}_2\,, \tag{B.6}$$

$$Z_\phi = 1+(\xi-3)g^2\mathcal{I}_2\,, \tag{B.7}$$

JHEP08(2025)109

we display the coefficients up to dimension-four operators *viz.*

$$\hat{g}_3^2 = g^2 T\Big[1 - \frac{1}{3}g^2\mathcal{I}_2\Big] \,, \tag{B.8}$$

$$\hat{\mu}_3^2 = \mu^2 + (dg^2 + 4\lambda)\mathcal{I}_1 \,, \tag{B.9}$$

$$\widehat{m}_{\rm D}^2 = 2(d-1)g^2\mathcal{I}_1 \,, \tag{B.10}$$

$$\hat{\lambda}_3 = \lambda\, T - \Big[dg^4 - 6g^2\lambda + 10\lambda^2\Big]\mathcal{I}_2\, T \,, \tag{B.11}$$

$$\hat{h}_3 = g^2\, T - \frac{1}{3}\Big[(2d-5)g^4 + 12(d-3)g^2\lambda\Big]\mathcal{I}_2\, T \,, \tag{B.12}$$

$$\hat{\kappa}_3 = -\frac{1}{6}(d-3)(d-1)g^4\mathcal{I}_2\, T \,. \tag{B.13}$$

Here and henceforth, we employ hatted coefficients (e.g. $\widehat{\alpha}_i$) for quantities before field redefinitions and un-hatted coefficients (e.g. α_i) for quantities after field redefinitions.

The novel dimension-six operator coefficients read

$$\widehat{\alpha}_{D^2F^2} = -\frac{1}{30}g^2\mathcal{I}_3 \,, \tag{B.14}$$

$$\widehat{\alpha}_{D^4B_0^2} = \frac{1}{30}(d-6)g^2\mathcal{I}_3 \,, \tag{B.15}$$

$$\widehat{\alpha}_{D^2B_0^4} = -\frac{1}{9}(d-5)(d-4)g^4\mathcal{I}_3\, T \,, \tag{B.16}$$

$$\widehat{\alpha}_{B_0^2F^2} = -\frac{1}{6}(d-5)g^4\mathcal{I}_3\, T \,, \tag{B.17}$$

$$\widehat{\alpha}_{B_0^6} = \frac{1}{45}(d-5)(d-3)(d-1)g^6\mathcal{I}_3\, T^2 \,, \tag{B.18}$$

$$\widehat{\alpha}_{D^4\phi^2} = -\frac{1}{3}(3\xi-5)g^2\mathcal{I}_3 \,, \tag{B.19}$$

$$\widehat{\alpha}_{D^2\phi^4,1} = \frac{1}{3}\Big[(15-2d)g^4 + 80g^2\lambda - 8\lambda^2\Big]\mathcal{I}_3\, T \,, \tag{B.20}$$

$$\widehat{\alpha}_{D^2\phi^4,2} = -\frac{1}{6}\Big[(2d+5)g^4 - 4(3\xi+5)g^2\lambda + 16\lambda^2\Big]\mathcal{I}_3\, T \,, \tag{B.21}$$

$$\widehat{\alpha}_{D^2\phi^2F} = \frac{4}{3}g^3\mathcal{I}_3\, T^{1/2} \,, \tag{B.22}$$

$$\widehat{\alpha}_{\phi^2F^2} = \frac{1}{6}\Big[7g^4 - 4g^2\lambda\Big]\mathcal{I}_3\, T \,, \tag{B.23}$$

$$\widehat{\alpha}_{D^2\phi^2B_0^2,1} = -\frac{1}{3}\Big[(d-2)g^4 + 4(d-6)g^2\lambda\Big]\mathcal{I}_3\, T \,, \tag{B.24}$$

$$\widehat{\alpha}_{D^2\phi^2B_0^2,2} = \frac{1}{6}\Big[3(d+2\xi-6)g^4 - 4(d-4)g^2\lambda\Big]\mathcal{I}_3\, T \,, \tag{B.25}$$

$$\widehat{\alpha}_{D^2\phi^2B_0^2,3} = \frac{1}{3}(d-4)\Big[7g^4 - 4g^2\lambda\Big]\mathcal{I}_3\, T \,, \tag{B.26}$$

$$\widehat{\alpha}_{\phi^4B_0^2} = \frac{4}{3}\Big[dg^6 + 3(d-\xi)g^4\lambda + (13d-63)g^2\lambda^2\Big]\mathcal{I}_3\, T^2 \,, \tag{B.27}$$

$$\widehat{\alpha}_{\phi^2B_0^4} = \frac{1}{3}\Big[(d(d-4)-3\xi)g^6 + 4(d-3)(d-5)g^4\lambda\Big]\mathcal{I}_3\, T^2 \,, \tag{B.28}$$

$$\widehat{\alpha}_{\phi^6} = \frac{4}{3}\Big[dg^6 - 3\xi g^2\lambda^2 + 28\lambda^3\Big]\mathcal{I}_3\, T^2 \,. \tag{B.29}$$

Some of these 6-point vertices exhibit evanescent operator terms, whose coefficients vanish

JHEP08(2025)109

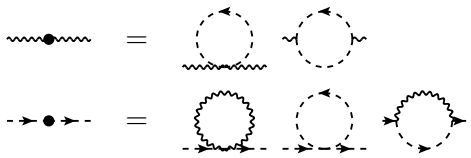

Figure 3. One-loop contributions to the Abelian Higgs model 2-point function at the soft EFT. Dashed directed lines denote soft scalars and wiggly lines soft spatial gauge fields. Diagrams are generated with `Axodraw` [131].

in $d = 3$, akin to the behavior observed in QCD [13]. Such operators can in general be eliminated through a shift of the operator basis [130].

The thermal master integrals used in this context have the form

$$\mathcal{I}_s^\alpha \;=\; \fint_P \frac{p_0^\alpha}{[P^2]^s} = 2T\frac{[2\pi T]^{d-2s+\alpha}}{(4\pi)^{\frac{d}{2}}}\frac{\Gamma(s-\frac{d}{2})}{\Gamma(s)}\zeta_{2s-\alpha-d}\,, \tag{B.30}$$

$$\mathcal{I}_3 \overset{d=3-2\epsilon}{=} \frac{\zeta_3\,\mu^{-2\epsilon}}{128\pi^4T^2}\biggl\{1+2\epsilon\biggl[\ln\Bigl(\frac{\bar{\Lambda}e^{\gamma_{\rm E}}}{4\pi T}\Bigr)+1-\gamma_{\rm E}+\frac{\zeta_3'}{\zeta_3}\biggr]+\mathcal{O}(\epsilon^2)\biggr\}\,, \tag{B.31}$$

where $\zeta_n \equiv \zeta(n)$ and $\mathcal{I}_s = \mathcal{I}_s^0$. Along the way, we utilized the one-loop integration-by-parts (IBP) identity

$$\mathcal{I}_{s+1}^{\alpha+2} = \Bigl(1-\frac{d}{2s}\Bigr)\mathcal{I}_s^\alpha\,. \tag{B.32}$$

B.3 Dimension-six vertices of the soft 3d EFT in the S/T basis

Below, we collect the results for dimension-six vertices and the corresponding mapping to the operator coefficients defined in the previous section.

Because the presence of a heat bath breaks Lorentz invariance, we need to introduce separate notation for spatial and zero spacetime indices akin to [13]. The full Kronecker symbol is denoted by

$$\delta_{\mu\nu} \;\equiv\; T_{\mu\nu}+S_{\mu\nu}\,,\quad T_{\mu\nu} \;\equiv\; \delta_{\mu0}\delta_{\nu0}\,,\quad S_{\mu\nu} \;\equiv\; \delta_{\mu i}\delta_{\nu i}\,. \tag{B.33}$$

We also introduce the totally symmetric tensors

$$T_{\mu\nu\rho\sigma} \equiv \delta_{\mu0}\delta_{\nu0}\delta_{\rho0}\delta_{\sigma0}\,, \tag{B.34}$$

$$T_{\mu\nu\rho\sigma\alpha\beta} \equiv \delta_{\mu0}\delta_{\nu0}\delta_{\rho0}\delta_{\sigma0}\delta_{\alpha0}\delta_{\beta0}\,, \tag{B.35}$$

$$\delta_{\mu\nu\rho\sigma} \equiv \delta_{\mu\nu}\delta_{\rho\sigma}+2\text{ permutations}\,, \tag{B.36}$$

$$\delta_{\mu\nu\rho\sigma\alpha\beta} \equiv \delta_{\mu\nu}\delta_{\rho\sigma}\delta_{\alpha\beta}+14\text{ permutations}\,. \tag{B.37}$$

It is advantageous to employ a basis in which the spatial and temporal indices are strictly separated from each other.

The 2-point vertex can be expressed as

$$\delta S_{\rm soft}^{(2)} = B_\mu(q)\,B_\nu(-q)\Bigl\{\eta_1\,q^2(q^2S_{\mu\nu}-q_\mu q_\nu)+\eta_2\,q^4T_{\mu\nu}\Bigr\}+\eta_3\,q^4\,\phi(q)\,\phi^\dagger(-q)\,. \tag{B.38}$$

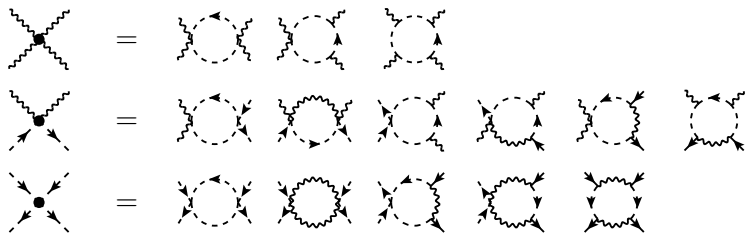

Figure 4. One-loop contributions to the Abelian Higgs model 4-point function at the soft EFT. Lines are defined in figure 3. Additional scalar line orientations are omitted for compactness.

Here and henceforth, for the matching coefficients in the action, field normalization is accounted for such that for a general correlator e.g. $\Gamma_{\phi_1\ldots,\phi_n} = \eta_{\phi_1\ldots\phi_n} Z_{\phi_1}^{\frac{1}{2}} \ldots Z_{\phi_n}^{\frac{1}{2}}$. The contributing 2-point diagrams are collected in figure 3. A representation of the coefficients was chosen to map directly into the $\widehat{\alpha}$ coefficients of section B.2,

$$\eta_1 = \widehat{\alpha}_{D^2F^2} \,, \qquad \eta_2 = \widehat{\alpha}_{D^4B_0^2} \,, \qquad \eta_3 = \widehat{\alpha}_{D^4\phi^2} \,. \tag{B.39}$$

The 4-point vertex can be expressed as

$$\begin{aligned}
\delta S^{(4)}_{\text{soft}} = \delta(q+r+s+t)\Big[& \\
& + B_\mu(q)\, B_\nu(r)\, B_\rho(s)\, B_\sigma(t) \left\{ \psi_1 (S_{\mu\nu} q\cdot r + q_\mu r_\nu)\, T_{\rho\sigma} + \psi_2\, q^2\, T_{\mu\nu\rho\sigma} \right\} \\
& + B_\mu(q)\, B_\nu(r)\, \phi(s)\, \phi^\dagger(t) \Big\{ \psi_3 \left(S_{\mu\nu} q^2 - q_\mu q_\nu\right) + \psi_4 \left(S_{\mu\nu} q\cdot r - q_\mu r_\nu\right) \\
& \qquad + \psi_5 \left(S_{\mu\nu}(s^2+t^2) - (q_\mu + 2t_\mu)(r_\mu + 2s_\nu)\right) \\
& \qquad + \left(\psi_6\, q^2 + \psi_7 \left(s^2+t^2\right) + \psi_8\, s\cdot t\right) T_{\mu\nu} \Big\} \\
& + \phi(q)\, \phi(r)\, \phi^\dagger(s)\, \phi^\dagger(t) \left\{ \psi_9 \left(q^2+s^2\right) + \psi_{10}\, q\cdot s \right\} \Big] \,,
\end{aligned} \tag{B.40}$$

where the contributing 4-point diagrams are collected in figure 4. Purely spatial contributions to the B_μ^4 correlator vanish identically after symmetry shifts and momentum conservation due to the Abelian nature of the theory. A representation of the coefficients can be chosen as

$$\begin{aligned}
&\psi_1 = -2\widehat{\alpha}_{B_0^2F^2} \,, \quad \psi_2 = -\widehat{\alpha}_{D^2B_0^4} \,, \quad \psi_3 = -\hat{g}_3\, \widehat{\alpha}_{D^2\phi^2F} \,, \quad \psi_4 = -2\widehat{\alpha}_{\phi^2F^2} \,, \\
&\psi_5 = \hat{g}_3^2\, \widehat{\alpha}_{D^4\phi^2} \,, \quad \psi_6 = -\widehat{\alpha}_{D^2\phi^2B_0^2,1} \,, \quad \psi_7 = -\widehat{\alpha}_{D^2\phi^2B_0^2,2} \,, \quad \psi_8 = -\widehat{\alpha}_{D^2\phi^2B_0^2,3} \,, \\
&\psi_9 = -\widehat{\alpha}_{D^2\phi^4,2} \,, \quad \psi_{10} = -\widehat{\alpha}_{D^2\phi^4,1} \,.
\end{aligned} \tag{B.41}$$

The 6-point vertex can be expressed as

$$\begin{aligned}
\delta S^{(6)}_{\text{soft}} = & \int_X B_\mu\, B_\nu\, B_\rho\, B_\sigma\, B_\alpha\, B_\beta \left\{ \chi_1\, S_{\mu\nu} S_{\rho\sigma} S_{\alpha\beta} + \chi_2\, S_{\mu\nu} S_{\rho\sigma} T_{\alpha\beta} + \chi_3\, S_{\mu\nu} T_{\rho\sigma\alpha\beta} + \chi_4\, T_{\mu\nu\rho\sigma\alpha\beta} \right\} \\
& + \int_X B_\mu\, B_\nu\, B_\rho\, B_\sigma\, \phi\, \phi^\dagger \left\{ \chi_5\, S_{\mu\nu} S_{\rho\sigma} + \chi_6\, S_{\mu\nu} T_{\rho\sigma} + \chi_7\, T_{\mu\nu\rho\sigma} \right\} \\
& + \int_X B_\mu\, B_\nu\, (\phi\, \phi^\dagger)^2 \left\{ \chi_8\, S_{\mu\nu} + \chi_9\, T_{\mu\nu} \right\} + \int_X (\phi\, \phi^\dagger)^3\, \chi_{10} \,,
\end{aligned} \tag{B.42}$$

JHEP08(2025)109

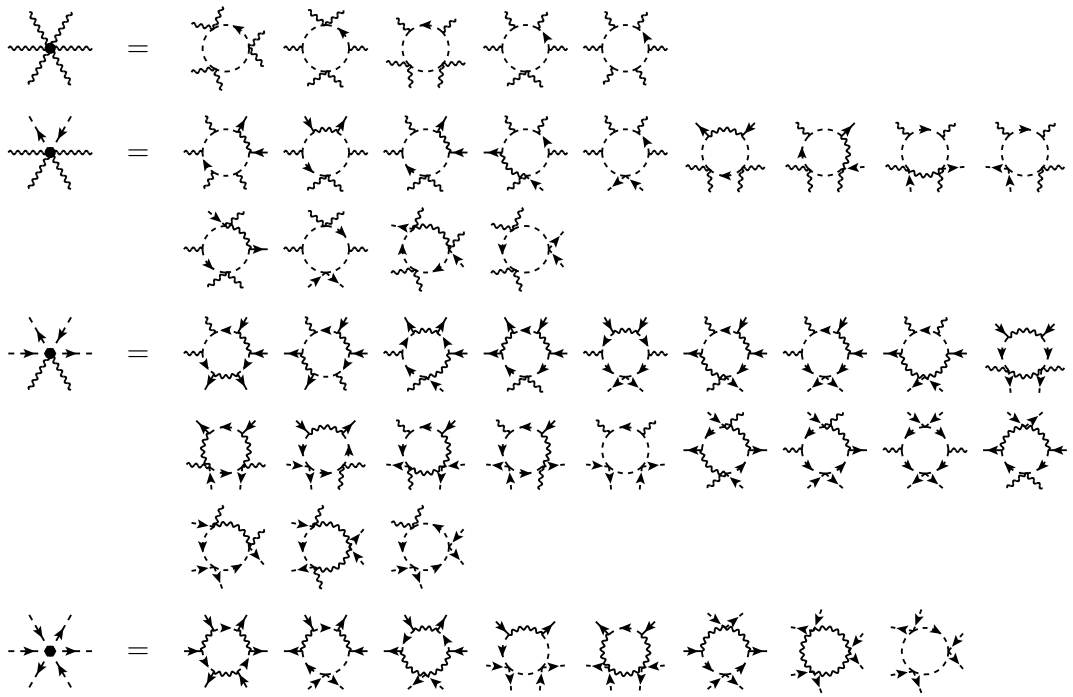

Figure 5. One-loop contributions to the Abelian Higgs model 6-point function at the soft EFT. Lines are defined in figure 3. Additional scalar line orientations are omitted for compactness.

where the contributing 6-point diagrams are collected in figure 5. While purely spatial contributions vanish, we present the relationship between the coefficients χ_i and $\widehat{\alpha}_i$:

$$\begin{aligned}
&\chi_1 = \chi_2 = \chi_3 = 0\,, && \chi_4 = \widehat{\alpha}_{B_0^6}\,, && \chi_5 = \hat{g}_3^4 \widehat{\alpha}_{D^4\phi^2}\,,\\
&\chi_6 = \hat{g}_3^2(\widehat{\alpha}_{D^2\phi^2 B_0^2,3} - 2\widehat{\alpha}_{D^2\phi^2 B_0^2,2})\,, && \chi_7 = \widehat{\alpha}_{B_0^4\phi^2}\,, && \chi_8 = \hat{g}_3^2(\widehat{\alpha}_{D^2\phi^4,1} - 2\widehat{\alpha}_{D^2\phi^4,2})\,,\\
&\chi_9 = \widehat{\alpha}_{B_0^2\phi^4}\,, && \chi_{10} = \widehat{\alpha}_{\phi^6}\,. &&
\end{aligned} \tag{B.43}$$

B.4 Lagrangian of the soft 3d EFT after field redefinitions

Below, we rewrite the most general 3d theory Lagrangian from eqs. (3.4) and (3.6),

$$\begin{aligned}
\mathcal{L}^{\rm 3d}_{\rm soft} = &\frac{1}{4}F_{ij}F_{ij} + (D_i\phi)^\dagger(D_i\phi) + \mu_3^2\phi^\dagger\phi + \lambda_3(\phi^\dagger\phi)^2\\
&+ \frac{1}{2}(\partial_i B_0)(\partial_i B_0) + h_3(\phi^\dagger\phi)B_0^2 + \frac{1}{2}m_{\rm D}^2 B_0^2 + \kappa_3 B_0^4\\
&+ \alpha_{\phi^2F^2}F_{ij}F_{ij}\phi^\dagger\phi + \alpha_{D^2\phi^4}\phi^\dagger\phi(D_i\phi)^\dagger(D_i\phi) + \alpha_{B_0^2F^2}B_0^2F_{ij}F_{ij} + \alpha_{D^2\phi^2B_0^2}\phi^\dagger\phi(\partial_i B_0)^2\\
&+ \alpha_{B_0^6}B_0^6 + \alpha_{\phi^2B_0^4}(\phi^\dagger\phi)B_0^4 + \alpha_{\phi^4B_0^2}(\phi^\dagger\phi)^2B_0^2 + \alpha_{\phi^6}(\phi^\dagger\phi)^3\,.
\end{aligned} \tag{B.44}$$

Here, we included operators up to dimension six in the physical basis, ensuring that redundant operators — those removable via field redefinitions — are excluded. Utilizing `Matchete` [116],

JHEP08(2025)109

the coefficients of the physical basis up to dimension four are given by

$$\mu_3^2 = \hat{\mu}_3^2(1 + \widehat{\alpha}_{D^4\phi^2}\hat{\mu}_3^2) \,, \tag{B.45}$$

$$m_{\rm D}^2 = \widehat{m}_{\rm D}^2(1 + 2\widehat{\alpha}_{D^4B_0^2}\widehat{m}_{\rm D}^2) \,, \tag{B.46}$$

$$\kappa_3 = \hat{\kappa}_3(1 + 8\widehat{m}_{\rm D}^2\widehat{\alpha}_{D^4B_0^2}) + \widehat{m}_{\rm D}^2\widehat{\alpha}_{D^2B_0^4} \,, \tag{B.47}$$

$$\begin{aligned} h_3 = {} & \hat{h}_3(1 + 4\widehat{m}_{\rm D}^2\widehat{\alpha}_{D^4B_0^2} + 2\hat{\mu}_3^2\widehat{\alpha}_{D^4\phi^2}) + \hat{\mu}_3^2(2\widehat{\alpha}_{D^2\phi^2B_0^2,2} - \widehat{\alpha}_{D^2\phi^2B_0^2,3}) \\ & + \widehat{m}_{\rm D}^2(\widehat{\alpha}_{D^2\phi^2B_0^2,1} + \widehat{\alpha}_{D^2\phi^2B_0^2,3}) \,, \end{aligned} \tag{B.48}$$

$$\lambda_3 = \hat{\lambda}_3(1 + 4\hat{\mu}_3^2\widehat{\alpha}_{D^4\phi^2}) + \hat{\mu}_3^2(2\hat{g}_3^2\widehat{\alpha}_{D^2F^2} + 2\widehat{\alpha}_{D^2\phi^4,2} + \hat{g}_3\widehat{\alpha}_{D^2\phi^2F}) \,, \tag{B.49}$$

where $g_3^2 = \hat{g}_3^2$. While these relations hold to all orders up to dimension-six operators, we effectively truncate them at NLO i.e. $\mathcal{O}(g^4)$ during the matching, omitting terms of $\mathcal{O}(g^6)$. Therefore dimension-six induced field redefinitions only start to affect the dimension-four Wilson coefficients at next-to-next-to-leading order (NNLO) which in particular corresponds to three-loop level for the effective masses and two-loop level for the effective couplings.

The non-renormalizable dimension-six derivative-operator coefficients

$$\alpha_{D^2\phi^2B_0^2} = \widehat{\alpha}_{D^2\phi^2B_0^2,3} \,, \tag{B.50}$$

$$\alpha_{B_0^2F^2} = \widehat{\alpha}_{B_0^2F^2} \,, \tag{B.51}$$

$$\alpha_{\phi^2F^2} = \widehat{\alpha}_{\phi^2F^2} \,, \tag{B.52}$$

$$\alpha_{D^2\phi^4} = \widehat{\alpha}_{D^2\phi^4,1} + 3\hat{g}_3\,\widehat{\alpha}_{D^2\phi^2F} + 6\hat{g}_3^2\,\widehat{\alpha}_{D^2F^2} \,, \tag{B.53}$$

are truncated at $\mathcal{O}(g^4)$. The field-redefined marginal dimension-six coefficients,

$$\alpha_{B_0^6} = \widehat{\alpha}_{B_0^6} + 4\hat{\kappa}_3(\widehat{\alpha}_{D^2B_0^4} + 4\hat{\kappa}_3\widehat{\alpha}_{D^4B_0^2}) \,, \tag{B.54}$$

$$\begin{aligned} \alpha_{\phi^2B_0^4} = {} & \widehat{\alpha}_{\phi^2B_0^4} + 4\hat{\kappa}_3(\widehat{\alpha}_{D^2\phi^2B_0^2,1} + \widehat{\alpha}_{D^2\phi^2B_0^2,3} + 4\hat{h}_3\widehat{\alpha}_{D^4B_0^2}) \\ & + \hat{h}_3(2\widehat{\alpha}_{D^2\phi^2B_0^2,2} - \widehat{\alpha}_{D^2\phi^2B_0^2,3} + 2\widehat{\alpha}_{D^2B_0^4}) + \hat{h}_3^2\widehat{\alpha}_{D^4\phi^2} \,, \end{aligned} \tag{B.55}$$

$$\begin{aligned} \alpha_{\phi^4B_0^2} = {} & \widehat{\alpha}_{\phi^4B_0^2} + 2\hat{\lambda}_3(2\widehat{\alpha}_{D^2\phi^2B_0^2,2} - \widehat{\alpha}_{D^2\phi^2B_0^2,3}) \\ & + 2\hat{h}_3(\widehat{\alpha}_{D^2\phi^2B_0^2,1} + \widehat{\alpha}_{D^2\phi^2B_0^2,3} + 2\hat{\lambda}_3\widehat{\alpha}_{D^4\phi^2} + \widetilde{\alpha}_{D^2\phi^4}) + 4\hat{h}_3^2\widehat{\alpha}_{D^4B_0^2} \,, \end{aligned} \tag{B.56}$$

$$\alpha_{\phi^6} = \widehat{\alpha}_{\phi^6} + 4\hat{\lambda}_3(\widetilde{\alpha}_{D^2\phi^4} + \hat{\lambda}_3\widehat{\alpha}_{D^4\phi^2}) \,, \tag{B.57}$$

are truncated at $\mathcal{O}(g^6)$, using

$$\widetilde{\alpha}_{D^2\phi^4} = \widehat{\alpha}_{D^2\phi^4,2} + \frac{1}{2}\hat{g}_3\,\widehat{\alpha}_{D^2\phi^2F} + \hat{g}_3^2\,\widehat{\alpha}_{D^2F^2} \,. \tag{B.58}$$

Below, we present the expressions for the previously defined α-coefficients both in general d and $d = 3 - 2\epsilon$ dimensions. Notably, these coefficients are entirely independent of the gauge-fixing parameter ξ, except for terms consistent with corrections arising from the matching of the two theories at the three-loop level. Therefore, in this basis, the gauge independence

JHEP08(2025)109

of physical observables is manifest, *viz.*

$$\begin{aligned}
\alpha_{B_0^6} &= \frac{1}{45}(d-5)(d-3)(d-1)g^6\mathcal{I}_3\,T^2+\mathcal{O}(g^8)\\
&\overset{d=3-2\epsilon}{=} \mathcal{O}(g^8)\,, &\text{(B.59)}\\
\alpha_{\phi^2B_0^4} &= \frac{1}{9}\Big[(d-5)(d-1)g^6+12(d-5)(d-3)g^4\lambda\Big]\mathcal{I}_3\,T^2+\mathcal{O}(g^8)\\
&\overset{d=3-2\epsilon}{=} -\frac{\zeta_3}{288\pi^4}g^6+\mathcal{O}(g^8)\,, &\text{(B.60)}\\
\alpha_{\phi^4B_0^2} &= \frac{2}{15}\Big[(36d-139)g^6+10(35-3d)g^4\lambda+10(13d-67)g^2\lambda^2\Big]\mathcal{I}_3\,T^2+\mathcal{O}(g^8)\\
&\overset{d=3-2\epsilon}{=} -\frac{\zeta_3}{960\,\pi^4}\Big(31\,g^6\ -260\,g^4\,\lambda+280\,g^2\,\lambda^2\Big)+\mathcal{O}(g^8)\,, &\text{(B.61)}\\
\alpha_{\phi^6} &= \frac{4}{15}\Big[5dg^6-(5d+3)g^4\lambda+75g^2\lambda^2+100\lambda^3\Big]\mathcal{I}_3\,T^2+\mathcal{O}(g^8)\\
&\overset{d=3-2\epsilon}{=} \frac{\zeta_3}{480\,\pi^4}\Big(15\,g^6-18\,g^4\,\lambda+75\,g^2\,\lambda^2+100\,\lambda^3\Big)+\mathcal{O}(g^8)\,, &\text{(B.62)}\\
\alpha_{D^2\phi^2B_0^2} &= \frac{1}{3}(d-4)\Big[7g^4-4g^2\,\lambda\Big]\mathcal{I}_3\,T+\mathcal{O}(g^6)\\
&\overset{d=3-2\epsilon}{=} -\frac{\zeta_3}{384\,\pi^4T}\Big(7\,g^4-4\,g^2\lambda\Big)+\mathcal{O}(g^6)\,, &\text{(B.63)}\\
\alpha_{B_0^2F^2} &= -\frac{1}{6}(d-5)g^4\,\mathcal{I}_3\,T+\mathcal{O}(g^6)\\
&\overset{d=3-2\epsilon}{=} \frac{\zeta_3}{384\pi^4T}g^4+\mathcal{O}(g^6)\,, &\text{(B.64)}\\
\alpha_{\phi^2F^2} &= \frac{1}{6}\Big[7g^4-4g^2\,\lambda\Big]\mathcal{I}_3\,T+\mathcal{O}(g^6)\\
&\overset{d=3-2\epsilon}{=} \frac{\zeta_3}{768\pi^4T}\Big(7\,g^4-4\,g^2\,\lambda\Big)+\mathcal{O}(g^6)\,, &\text{(B.65)}\\
\alpha_{D^2\phi^4} &= \frac{2}{15}\Big[(66-5d)g^4+200g^2\,\lambda-20\lambda^2\Big]\mathcal{I}_3\,T+\mathcal{O}(g^6)\\
&\overset{d=3-2\epsilon}{=} \frac{\zeta_3}{960\pi^4T}\Big(51\,g^4+200\,g^2\,\lambda-20\,\lambda^2\Big)+\mathcal{O}(g^6)\,, &\text{(B.66)}
\end{aligned}$$

where

$$L_b\equiv 2\ln\frac{\bar{\Lambda}}{T}-2\big(\ln(4\pi)-\gamma_{\rm E}\big)\,. \tag{B.67}$$

After performing field redefinitions, the Wilson coefficients are not completely gauge-independent, as the dimension-four coefficients μ_3^2, h_3, and λ_3, still contain terms proportional to ξ. However, these gauge-dependent terms are of the same order as the corrections arising from three-loop dimensional reduction.[13] This suggests that such higher-order corrections may further cancel the residual ξ-dependence. The matching relations in $d=3-2\epsilon$ up to

[13]This conclusion also holds for the three-loop dimensional reduction matching of the dimension-six operator coefficients $\alpha_{\phi^2B_0^4}$, $\alpha_{\phi^4B_0^2}$, and α_{ϕ^6} which is of $\mathcal{O}(g^{10})$.

JHEP08(2025)109

$\mathcal{O}(g^6)$ for the scalar and Debye masses, are given by

$$
\begin{aligned}
\mu_3^2 &= \Big[\mu^2\Big]_{\text{tree level}} + T^2\Big[\frac{1}{3}\lambda + \frac{1}{4}g^2\Big]_{\text{1loop}} - \Big[\Big(\mu^2 + \frac{1}{4}g^2\,T^2 + \frac{1}{3}\lambda T^2\Big)\delta Z_\phi\Big]_{\text{2loop}} \\
&\quad + \frac{T^2}{(4\pi)^2}\Big[- \frac{8+39L_b}{36}g^4 + \frac{2(1+3L_b)}{3}\,g^2\lambda - \frac{10}{3}L_b\,\lambda^2 + (3\,g^2 - 4\,\lambda)L_b\frac{\mu^2}{T^2} \\
&\qquad + (-8\lambda^2 - 6g^4 + 8g^2\lambda)\Big(c + \ln\frac{3T}{\bar{\Lambda}}\Big) + \frac{4\,g_3^4 + 8\,\lambda_3^2 + 2h_3^2 - 8g_3^2\,\lambda_3}{T^2}\ln\frac{\bar{\Lambda}_{\text{3d}}}{\bar{\Lambda}}\Big]_{\text{2loop}} \\
&\quad + \frac{T^2}{(4\pi)^4}\Big[\frac{L_b(216\,c_1 - 16 + 138L_b) + 5\zeta_3}{24}g^6 - \frac{L_b(108\,c_1 - 18 + 54L_b) - 5\,\zeta_3}{9}g^4\lambda \\
&\qquad + \frac{2(162\,c_1\,L_b + 27L_b^2 + 5\zeta_3)}{27}g^2\lambda^2 + \frac{(27L_b^2 + 5\zeta_3)g^2 - 4(27L_b^2 - 5\zeta_3)\lambda}{3}g^2\frac{\mu^2}{T^2} \\
&\qquad + \frac{10\zeta_3}{3}g^2\frac{\mu^4}{T^4} + \xi\,\mathcal{C}^{\xi}_{\mu_3}\Big]_{\text{FR}} + \Big[\delta\mu_3^2\Big]_{\text{3loop}} + \mathcal{O}(g^8)\,, \qquad \text{(B.68)} \\
m_{\text{D}}^2 &= \Big[\frac{1}{3}g^2\,T^2\Big]_{\text{1loop}} + \frac{g^2T^2}{(4\pi)^2}\Big[\frac{7 - L_b}{9}\,g^2 + \frac{4}{3}\Big(\lambda + 3\frac{\mu^2}{T^2}\Big)\Big]_{\text{2loop}} + \Big[\delta m_{\text{D}}^2\Big]_{\text{3loop}} \\
&\quad + \frac{g^4T^2}{(4\pi)^4}\Big[\frac{5L_b^2 - 25L_b - 70 - 6\zeta_3}{135}\,g^2 - \frac{4(L_b+2)}{9}\Big(\lambda + 3\frac{\mu^2}{T^2}\Big)\Big]_{\text{FR}} + \mathcal{O}(g^8)\,, \qquad \text{(B.69)}
\end{aligned}
$$

where terms arising through a field redefinition (FR) are indicated explicitly. From eq. (B.69), one can directly infer the gauge-independence of the Debye mass at three-loop level; see the QCD Debye mass [132]. The soft EFT couplings are

$$
\begin{aligned}
g_3^2 &= \Big[g^2\,T\Big]_{\text{tree level}} - \frac{g^4T}{(4\pi)^2}\Big[\frac{L_b}{3}\Big]_{\text{1loop}} + \Big[\delta g_3^2 - g^2T\,\delta Z_{B_i}\Big]_{\text{2loop}} + \mathcal{O}(g^8)\,, \qquad \text{(B.70)} \\
\kappa_3 &= \frac{T}{(4\pi)^2}\Big[\frac{2}{3}g^4\Big]_{\text{1loop}} - \frac{T}{(4\pi)^4}\Big[\frac{4\zeta_3}{27}g^6\Big]_{\text{FR}} + \Big[\delta\kappa_3\Big]_{\text{2loop}} + \mathcal{O}(g^8)\,, \qquad \text{(B.71)} \\
h_3 &= \Big[g^2\,T\Big]_{\text{tree level}} + \frac{T}{(4\pi)^2}\Big[\frac{4 - L_b}{3}g^4 + 8\,g^2\lambda\Big]_{\text{1loop}} + \Big[\delta h_3 - g^2T(\delta Z_{B_0} + \delta Z_\phi)\Big]_{\text{2loop}} \\
&\quad + \frac{\zeta_3 T}{(4\pi)^4}\frac{16}{45}\Big[- 2\,g^6 + 15\,g^4\Big(\lambda + \frac{\mu^2}{T^2}\Big)\Big]_{\text{FR}} + \mathcal{O}(g^8)\,, \qquad \text{(B.72)} \\
\lambda_3 &= \Big[\lambda\,T\Big]_{\text{tree level}} + \frac{T}{(4\pi)^2}\Big[(2 - 3L_b)\,g^4 + 6\,L_b\,g^2\lambda - 10\,L_b\,\lambda^2\Big]_{\text{1loop}} + \Big[\delta\lambda_3 - 2\lambda T\,\delta Z_\phi\Big]_{\text{2loop}} \\
&\quad + \frac{\zeta_3 T}{(4\pi)^4}\Big[- \frac{6}{5}\Big(g^2 + 4\frac{\mu^2}{T^2}\Big)\,g^4 + \frac{76}{15}g^4\lambda + \frac{56}{9}g^2\lambda^2 - \frac{32}{9}\Big(\lambda + 3\frac{\mu^2}{T^2}\Big)\lambda^2 + \frac{80}{3}g^2\lambda\,\frac{\mu^2}{T^2}\Big]_{\text{FR}} \\
&\quad + \mathcal{O}(g^8)\,, \qquad \text{(B.73)}
\end{aligned}
$$

which are gauge-independent at the given two-loop level. Here, $c \equiv \frac{1}{2}(\ln\frac{8\pi}{9} + (\ln\zeta_2)' - 2\gamma_{\text{E}})$, $c_1 \equiv \ln(2\pi) - (\ln\zeta_2)'$. We also introduced, $\delta\mu_3^2$ as the scalar and δm_{D}^2 as the Debye mass three-loop contribution including their 3d running. The coefficients δZ_ϕ, δZ_{B_0}, $\delta\kappa_3$, δh_3, $\delta\lambda_3$ are the two-loop contributions to Z_ϕ, Z_{B_0}, κ_3, h_3, λ_3 including their 3d running, while

JHEP08(2025)109

dimension 2	
$\phi^\dagger\phi$	$\bar{Z}_\phi\,\hat{\bar{\mu}}_3^2$

dimension 4	
$F_{ij}F_{ij}/4$	$\bar{Z}_{B_i}$
$(D_i\phi)^\dagger(D_i\phi)$	$\bar{Z}_\phi$
$(\phi^\dagger\phi)^2$	$\bar{Z}_\phi^2\,\widehat{\bar{\alpha}}_{\phi^4}$

dimension 6	
$(\partial_i F_{ij})^2$	$\bar{Z}_{B_i}\,\widehat{\bar{\alpha}}_{D^2F^2}$
$(D^2\phi^\dagger)(D^2\phi)$	$\bar{Z}_\phi\,\widehat{\bar{\alpha}}_{D^4\phi^2}$
$(\phi^\dagger\phi)(D_i\phi^\dagger D_i\phi)$	$\bar{Z}_\phi^2\,\widehat{\bar{\alpha}}_{D^2\phi^4,1}$
$(\phi^\dagger\phi)(\phi^\dagger D^2\phi + h.c.)$	$\bar{Z}_\phi^2\,\widehat{\bar{\alpha}}_{D^2\phi^4,2}$
$(\partial_i F_{ij})i\phi^\dagger(D_j\phi)$	$\bar{Z}_\phi\bar{Z}_{B_i}^{1/2}\,\widehat{\bar{\alpha}}_{D^2\phi^2F}$
$F_{ij}F_{ij}\phi^\dagger\phi$	$\bar{Z}_{B_i}\bar{Z}_\phi\,\widehat{\bar{\alpha}}_{\phi^2F^2}$
$(\phi^\dagger\phi)^3$	$\bar{Z}_\phi^3\,\widehat{\bar{\alpha}}_{\phi^6}$

Table 4. All possible dimension-six operators in the softer-scale 3d effective theory.

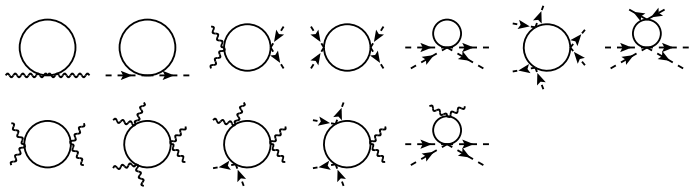

Figure 6. One-loop contributions to the Abelian Higgs model 2-point, 4-point and 6-point functions at the softer EFT. Dashed directed lines denote softer scalars, wiggly lines softer spatial gauge fields, and solid lines temporal scalars B_0. Additional scalar line orientations are omitted for compactness. The diagrams listed in the second row contribute only to operators in the softer theory that are beyond dimension six.

the residual gauge dependent part corresponds to

$$\mathcal{C}^{\xi}_{\mu_3} \equiv -\frac{L_b(216\,c_1 - 16 + 138L_b) + 9\zeta_3}{72}g^6 + \frac{L_b(12\,c_1 - 2 + 6L_b) - \zeta_3}{3}g^4\lambda - \frac{2(18\,c_1L_b + 3L_b^2 + \zeta_3)}{9}g^2\lambda^2 - \Big[(3L_b^2+\zeta_3)g^2 - \frac{4(3L_b^2-\zeta_3)}{3}\lambda\Big]g^2\frac{\mu^2}{T^2} - 2\zeta_3 g^2\frac{\mu^4}{T^4}\,. \tag{B.74}$$

C Softer-scale EFT

Our goal now is to integrate out the soft scale and especially the massive field B_0. The interactions between the Higgs and spatial gauge fields, including all terms up to dimension-six operators, are summarized in table 4. Here, the covariant derivative is defined as $D_i \equiv \partial_i - i\bar{g}_3\bar{Z}_{B_i}^{1/2}B_i$. To this end, we determine the softer EFT coefficients at the full one-loop level, following the same approach as for the soft EFT in section B.3. The contributing diagrams are collected in figure 6.

The expressions for the dimension-four coefficients of the one-loop matching read

$$\hat{\bar{g}}_3^2 = g_3^2\Big[1 - 4\alpha_{B_0^2F^2}I_1\Big]\,, \tag{C.1}$$

$$\hat{\bar{\mu}}_3^2 = \mu_3^2 + \Big[h_3 - m_{\rm D}^2\alpha_{D^2\phi^2B_0^2}\Big]\,I_1\,, \tag{C.2}$$

$$\hat{\bar{\lambda}}_3 = \lambda_3 + \Big[-h_3^2 - \frac{2}{d-2}m_{\rm D}^2\alpha_{\phi^4B_0^2} + \frac{2d}{d-2}h_3m_{\rm D}^2\alpha_{D^2\phi^2B_0^2} - \frac{d+2}{d-2}m_{\rm D}^4\alpha^2_{D^2\phi^2B_0^2}\Big]I_2\,. \tag{C.3}$$

JHEP08(2025)109

In the corresponding field normalizations, only the spatial gauge bosons receive a non-trivial one-loop contribution at $\mathcal{O}(g^5)$,

$$\bar{Z}_{B_i} = 1 + 4\alpha_{B_0^2F^2} I_1 \,, \qquad\qquad \bar{Z}_\phi = 1 \,. \tag{C.4}$$

In this context, we also defined the 3d one-loop master integrals

$$I_\beta^\alpha(m^2) = \int_{\mathbf{p}} \frac{(p^2)^\alpha}{(p^2+m^2)^\beta} = m^{d+2(\alpha-\beta)} \frac{\Gamma(\alpha+\frac{d}{2})\Gamma(\beta-\alpha-\frac{d}{2})}{(4\pi)^{\frac{d}{2}}\,\Gamma(\beta)\Gamma(\frac{d}{2})} \,, \tag{C.5}$$

where $\int_{\mathbf{p}} = \int \frac{\mathrm{d}^d p}{(2\pi)^d}$, $I_\alpha \equiv I_\alpha^0(m_{\mathrm{D}}^2)$. Explicitly, one has

$$\begin{aligned} I_1 &\overset{d=3-2\epsilon}{=} -\frac{m_{\mathrm{D}}}{4\pi} + \mathcal{O}(\epsilon) \,, \\ I_2 &\overset{d=3-2\epsilon}{=} \frac{m_{\mathrm{D}}^{-1}}{8\pi} + \mathcal{O}(\epsilon) \,, \\ I_3 &\overset{d=3-2\epsilon}{=} \frac{m_{\mathrm{D}}^{-3}}{32\pi} + \mathcal{O}(\epsilon) \,, \end{aligned} \tag{C.6}$$

or can use the IBP identity

$$I_{s+1}(m^2) = \Big(1 - \frac{d}{2s}\Big) \frac{1}{m^2} I_s(m^2) \,. \tag{C.7}$$

For determining the dimension-six coefficients and since the softer Wilson coefficients originate from the purely spatial part of the Lagrangian, the mappings in eqs. (B.39), (B.41), and (B.43) can be directly reused. For the 2-point correction, we obtain a vanishing result

$$\bar{\eta}_1 = 0 \,, \qquad\qquad \bar{\eta}_3 = 0 \,, \tag{C.8}$$

since only for the non-Abelian case, cubic vertices between gauge fields can generate a 2-point $\mathcal{O}(k^4)$ contribution, and since the soft-theory coefficients $\alpha_{D^2F^2}$ and $\alpha_{D^4\phi^2}$ vanish in their physical basis (B.44) after field redefinitions.[14]

For the 4-point contributions to the action, the result reads

$$\bar{\psi}_1 = \bar{\psi}_3 = \bar{\psi}_5 = 0 \,, \tag{C.9}$$

$$\bar{\psi}_4 = -2\alpha_{\phi^2F^2} + 16\bigg[-\frac{1}{d-4} h_3 m_{\mathrm{D}}^2 \alpha_{B_0^2F^2} + \frac{d}{(d-2)(d-4)} m_{\mathrm{D}}^4 \alpha_{B_0^2F^2}\alpha_{D^2\phi^2B_0^2}\bigg] I_3 \,, \tag{C.10}$$

$$\bar{\psi}_9 = \bigg[\frac{1}{3}h_3^2 - \frac{2}{3}\frac{d+2}{d-4} h_3 m_{\mathrm{D}}^2 \alpha_{D^2\phi^2B_0^2} + \frac{1}{3}\frac{d^2+6d-4}{(d-2)(d-4)} m_{\mathrm{D}}^4 \alpha_{D^2\phi^2B_0^2}^2\bigg] I_3 \,, \tag{C.11}$$

$$\bar{\psi}_{10} = -\alpha_{D^2\phi^4} + 2\bar{\psi}_9 \,. \tag{C.12}$$

[14] In the matching of EQCD and MQCD [13], these coefficients have been kept in the soft EFT and introduced effective 2-point vertices. By employing field redefinitions, however, the effect of these 2-point vertices can be absorbed by the other Wilson coefficients.

JHEP08(2025)109

For the 6-point contributions to the action, the result reads

$$\bar{\chi}_1 = \bar{\chi}_5 = 0\,, \tag{C.13}$$

$$\bar{\chi}_8 = g_3^2 \alpha_{D^2\phi^4}\,, \tag{C.14}$$

$$\begin{aligned}\bar{\chi}_{10} = \alpha_{\phi^6} + 4\Big[&\frac{1}{3}h_3^3 - \frac{2dm_{\rm D}^4}{(d-2)(d-4)}\alpha_{\phi^4 B_0^2}\alpha_{D^2\phi^2 B_0^2} + \frac{2m_{\rm D}^2}{d-4}h_3\alpha_{\phi^4 B_0^2} - \frac{dm_{\rm D}^2}{d-4}h_3^2\alpha_{D^2\phi^2 B_0^2} \\ &+ \frac{d(d+2)}{(d-2)(d-4)}h_3 m_{\rm D}^4\alpha_{D^2\phi^2 B_0^2}^2 - \frac{1}{3}\frac{(d+2)(d+4)}{(d-2)(d-4)}m_{\rm D}^6\alpha_{D^2\phi^2 B_0^2}^3\Big] I_3\,.\end{aligned} \tag{C.15}$$

Here, the hard contributions are $\delta\bar{\eta}_i = \eta_i$, $\delta\bar{\psi}_i = \psi_i$, $\delta\bar{\chi}_i = \chi_i$.

In the following, we truncate the Wilson coefficients from the matching above at the corresponding orders in a power counting in the gauge coupling, g, of the fundamental 4d theory using eq. (3.12). This way, we exclude orders of

$$\begin{aligned}&\mathcal{O}(g^4)\,, && \text{for masses:} && \hat{\bar{\mu}}_3^2\,,\\ &\mathcal{O}(g^4)\,, && \text{for relevant couplings:} && \hat{\bar{\lambda}}_3^2\,, \hat{\bar{g}}_3^2\,,\\ &\mathcal{O}(g^4)\,, && \text{for marginal Wilson coefficients:} && \widehat{\bar{\alpha}}_{\phi^6}\,,\\ &\mathcal{O}(g^2)\,, && \text{for non-renormalizable Wilson coefficients:} && \widehat{\bar{\alpha}}_{D^2F^2}\,, \widehat{\bar{\alpha}}_{D^4\phi^2}\,, \widehat{\bar{\alpha}}_{D^2\phi^4,1}\,,\\ &&&&& \widehat{\bar{\alpha}}_{D^2\phi^4,2}\,, \widehat{\bar{\alpha}}_{D^2\phi^2F}\,, \widehat{\bar{\alpha}}_{\phi^2F^2}\,.\end{aligned} \tag{C.16}$$

The corresponding coefficients of the one-loop matching read, for the field normalizations,

$$\bar{Z}_{B_i} = 1 + \mathcal{O}(g^4)\,, \qquad\qquad \bar{Z}_\phi = 1\,, \tag{C.17}$$

and for the dimension-four coefficients,

$$\hat{\bar{\mu}}_3^2 = \mu_3^2 + h_3\, I_1 + \mathcal{O}(g^4)\,, \tag{C.18}$$

$$\hat{\bar{g}}_3^2 = g_3^2 + \mathcal{O}(g^4)\,, \tag{C.19}$$

$$\hat{\bar{\lambda}}_3 = \lambda_3 - h_3^2\, I_2 + \mathcal{O}(g^4)\,. \tag{C.20}$$

For $\hat{\bar{\lambda}}_3$ soft one-loop corrections are parametrically larger than hard one-loop correction. By employing the one-loop computations detailed below eq. (C.1) together with the mappings, eqs. (B.39), (B.41), and (B.43), the novel dimension-six operator coefficients, $\widehat{\bar{\alpha}}$, before field redefinitions are

$$\widehat{\bar{\alpha}}_{D^2F^2} = 0\,, \tag{C.21}$$

$$\widehat{\bar{\alpha}}_{D^4\phi^2} = 0\,, \tag{C.22}$$

$$\widehat{\bar{\alpha}}_{D^2\phi^4,1} = \alpha_{D^2\phi^4} - \frac{2}{3}\,h_3^2\, I_3 + \mathcal{O}(g^2)\,, \tag{C.23}$$

$$\widehat{\bar{\alpha}}_{D^2\phi^4,2} = -\frac{1}{3}\,h_3^2\, I_3 + \mathcal{O}(g^2)\,, \tag{C.24}$$

$$\widehat{\bar{\alpha}}_{D^2\phi^2F} = 0\,, \tag{C.25}$$

$$\widehat{\bar{\alpha}}_{\phi^2F^2} = \alpha_{\phi^2F^2} + \mathcal{O}(g^2)\,, \tag{C.26}$$

$$\widehat{\bar{\alpha}}_{\phi^6} = \alpha_{\phi^6} + \frac{4}{3}\,h_3^3\, I_3 + \mathcal{O}(g^4)\,. \tag{C.27}$$

JHEP08(2025)109

The Lagrangian in the physical basis is defined in eq. (3.16). From the redefinition of fields previously outlined in the dimensional reduction procedure (cf. section B.4), we can deduce the expression for the coefficients in the physical basis for operators up to dimension four *viz.*

$$\begin{aligned}
\bar{\mu}_3^2 &= \mu_3^2 + h_3\, I_1 + \mathcal{O}(g^4) \\
&\overset{d=3-2\epsilon}{=} \mu_3^2 - \frac{1}{4\pi}\, m_{\rm D}\, h_3 + \mathcal{O}(g^4) \\
&= \mu^2 + T^2\Big[\frac{1}{4}g^2 + \frac{1}{3}\lambda\Big]_{\rm DR} + T^2\Big[-\frac{1}{4\sqrt{3}\pi}g^3\Big]_{\rm SS} + \mathcal{O}(g^4)\,, \qquad \text{(C.28)} \\
\bar{\lambda}_3 &= \lambda_3 - h_3^2\, I_2 - \frac{2}{3}\Big(h_3 I_1 + \mu_3^2\Big) h_3^2 I_3 + \mathcal{O}(g^5) \\
&\overset{d=3-2\epsilon}{=} \lambda_3 - \frac{1}{8\pi}\frac{h_3^2}{m_{\rm D}} + \frac{1}{192\pi^2}\frac{h_3^3}{m_{\rm D}^2} - \frac{1}{48\pi}\frac{\mu_3^2\, h_3^2}{m_{\rm D}^3} + \mathcal{O}(g^5) \\
&= \lambda T + \frac{T}{(4\pi)^2}\Big[(2-3L_b)g^4 + 6L_b\, g^2\,\lambda - 10L_b\,\lambda^2\Big]_{\rm DR} \\
&\quad + T\Big[-\frac{1}{64\sqrt{3}\pi}\Big(27\, g^3 + 4\, g\,\lambda + 12\, g\,\frac{\mu^2}{T^2}\Big) + \frac{1}{64\pi^2}\, g^4\Big]_{\rm SS} + \mathcal{O}(g^4)\,, \qquad \text{(C.29)}
\end{aligned}$$

where $\bar{g}_3^2 = \hat{\bar{g}}_3^2$ and where, due to the truncation (C.16), we do not include the two-loop correction to $\bar{\mu}_3$ from eq. (3.19). And for operators of dimension six

$$\begin{aligned}
\overline{\alpha}_{D^2\phi^4} &= \alpha_{D^2\phi^4} - \frac{2}{3}\, h_3^2\, I_3 + \mathcal{O}(g^2) \\
&\overset{d=3-2\epsilon}{=} \alpha_{D^2\phi^4} - \frac{1}{48\pi}\frac{h_3^2}{m_{\rm D}^3} + \mathcal{O}(g^2) \\
&= \frac{\zeta_3 T}{960\pi^4}\Big[51\, g^4 + 200\, g^2\lambda - 20\,\lambda^2\Big]_{\rm DR} \\
&\quad + \frac{1}{T}\Big[-\frac{\sqrt{3}}{16\pi}\, g + \frac{1}{128\sqrt{3}\,\pi^3}\Big((L_b-4)g^3 - 24\, g\,\lambda\Big)\Big]_{\rm SS} + \mathcal{O}(g^2)\,, \qquad \text{(C.30)} \\
\overline{\alpha}_{\phi^2 F^2} &= \alpha_{\phi^2 F^2} + \mathcal{O}(g^2) \\
&\overset{d=3-2\epsilon}{=} \frac{\zeta_3}{768\pi^4}\frac{1}{T}\Big[7\, g^4 - 4\, g^2\lambda\Big]_{\rm DR} + \mathcal{O}(g^2)\,, \qquad \text{(C.31)} \\
\overline{\alpha}_{\phi^6} &= \alpha_{\phi^6} + \frac{4}{3}h_3^2\Big(h_3^2\, I_2 - \lambda_3 + h_3\Big) I_3 + \mathcal{O}(g^4) \\
&\overset{d=3-2\epsilon}{=} \alpha_{\phi^6} + \frac{1}{24\pi}\Big(h_3 - \lambda_3\Big)\frac{h_3^2}{m_{\rm D}^3} + \frac{1}{192\pi^2}\frac{h_3^4}{m_{\rm D}^4} + \mathcal{O}(g^4) \\
&= \frac{\zeta_3}{480\,\pi^4}\Big[15\, g^6 - 18\, g^4\lambda + 75\, g^2\lambda^2 + 100\,\lambda^3\Big]_{\rm DR} \\
&\quad + \Big[\frac{\sqrt{3}g}{8\,\pi}\Big(g^2 - \lambda\Big) + \frac{3}{64\pi^2}g^4 \\
&\quad + \frac{g}{\sqrt{3}(4\pi)^3}\Big(3(L_b+1)\, g^4 - 8(L_b-4)g^2\lambda + (15L_b-24)\lambda^2\Big) \\
&\quad - \frac{g^4}{(4\pi)^4}\Big((L_b-4)g^2 - 24\lambda\Big)\Big]_{\rm SS} + \mathcal{O}(g^4)\,. \qquad \text{(C.32)}
\end{aligned}$$

Contributions labelled DR (dimensional reduction) come from the hard modes and SS (soft scale) come from integrating out B_0.

JHEP08(2025)109

Data Availability Statement. The datasets supporting figures 1 and 2 are publicly available at [133].

Code Availability Statement. This article has no associated code or the code will not be deposited.

References

[1] K. Kajantie, M. Laine, K. Rummukainen and M.E. Shaposhnikov, *Is there a hot electroweak phase transition at $m_H \gtrsim m_W$?*, *Phys. Rev. Lett.* **77** (1996) 2887 [hep-ph/9605288] [INSPIRE].

[2] K. Kajantie, M. Laine, K. Rummukainen and M.E. Shaposhnikov, *A nonperturbative analysis of the finite T phase transition in SU(2) x U(1) electroweak theory*, *Nucl. Phys. B* **493** (1997) 413 [hep-lat/9612006] [INSPIRE].

[3] M. Gurtler, E.-M. Ilgenfritz and A. Schiller, *Where the electroweak phase transition ends*, *Phys. Rev. D* **56** (1997) 3888 [hep-lat/9704013] [INSPIRE].

[4] F. Csikor, Z. Fodor and J. Heitger, *Endpoint of the hot electroweak phase transition*, *Phys. Rev. Lett.* **82** (1999) 21 [hep-ph/9809291] [INSPIRE].

[5] M. D'Onofrio and K. Rummukainen, *Standard model cross-over on the lattice*, *Phys. Rev. D* **93** (2016) 025003 [arXiv:1508.07161] [INSPIRE].

[6] LISA Cosmology Working Group collaboration, *Cosmology with the Laser Interferometer Space Antenna*, *Living Rev. Rel.* **26** (2023) 5 [arXiv:2204.05434] [INSPIRE].

[7] K. Kajantie, M. Laine, K. Rummukainen and M.E. Shaposhnikov, *Generic rules for high temperature dimensional reduction and their application to the standard model*, *Nucl. Phys. B* **458** (1996) 90 [hep-ph/9508379] [INSPIRE].

[8] E. Braaten and A. Nieto, *Effective field theory approach to high temperature thermodynamics*, *Phys. Rev. D* **51** (1995) 6990 [hep-ph/9501375] [INSPIRE].

[9] K. Kajantie, M. Laine, K. Rummukainen and M.E. Shaposhnikov, *High temperature dimensional reduction and parity violation*, *Phys. Lett. B* **423** (1998) 137 [hep-ph/9710538] [INSPIRE].

[10] G.D. Moore, *Fermion determinant and the sphaleron bound*, *Phys. Rev. D* **53** (1996) 5906 [hep-ph/9508405] [INSPIRE].

[11] S. Chapman, *A new dimensionally reduced effective action for QCD at high temperature*, *Phys. Rev. D* **50** (1994) 5308 [hep-ph/9407313] [INSPIRE].

[12] N.P. Landsman, *Limitations to Dimensional Reduction at High Temperature*, *Nucl. Phys. B* **322** (1989) 498 [INSPIRE].

[13] M. Laine, P. Schicho and Y. Schröder, *Soft thermal contributions to 3-loop gauge coupling*, *JHEP* **05** (2018) 037 [arXiv:1803.08689] [INSPIRE].

[14] T. Gorda et al., *Three-dimensional effective theories for the two Higgs doublet model at high temperature*, *JHEP* **02** (2019) 081 [arXiv:1802.05056] [INSPIRE].

JHEP08(2025)109

[15] J.O. Andersen et al., *Nonperturbative Analysis of the Electroweak Phase Transition in the Two Higgs Doublet Model*, *Phys. Rev. Lett.* **121** (2018) 191802 [arXiv:1711.09849] [INSPIRE].

[16] K. Kainulainen et al., *On the validity of perturbative studies of the electroweak phase transition in the Two Higgs Doublet model*, *JHEP* **06** (2019) 075 [arXiv:1904.01329] [INSPIRE].

[17] O. Gould et al., *Nonperturbative analysis of the gravitational waves from a first-order electroweak phase transition*, *Phys. Rev. D* **100** (2019) 115024 [arXiv:1903.11604] [INSPIRE].

[18] L. Niemi, P. Schicho and T.V.I. Tenkanen, *Singlet-assisted electroweak phase transition at two loops*, *Phys. Rev. D* **103** (2021) 115035 [*Erratum ibid.* **109** (2024) 039902] [arXiv:2103.07467] [INSPIRE].

[19] L. Niemi, M.J. Ramsey-Musolf and G. Xia, *Nonperturbative study of the electroweak phase transition in the real scalar singlet extended standard model*, *Phys. Rev. D* **110** (2024) 115016 [arXiv:2405.01191] [INSPIRE].

[20] L. Niemi and T.V.I. Tenkanen, *Investigating two-loop effects for first-order electroweak phase transitions*, *Phys. Rev. D* **111** (2025) 075034 [arXiv:2408.15912] [INSPIRE].

[21] L. Niemi et al., *Electroweak phase transition in the real triplet extension of the SM: dimensional reduction*, *Phys. Rev. D* **100** (2019) 035002 [arXiv:1802.10500] [INSPIRE].

[22] J.E. Camargo-Molina, R. Enberg and J. Löfgren, *A new perspective on the electroweak phase transition in the Standard Model Effective Field Theory*, *JHEP* **10** (2021) 127 [arXiv:2103.14022] [INSPIRE].

[23] E. Camargo-Molina, R. Enberg and J. Löfgren, *A Catalog of First-Order Electroweak Phase Transitions in the Standard Model Effective Field Theory*, arXiv:2410.23210 [INSPIRE].

[24] D. Croon et al., *Theoretical uncertainties for cosmological first-order phase transitions*, *JHEP* **04** (2021) 055 [arXiv:2009.10080] [INSPIRE].

[25] M. Kierkla, B. Swiezewska, T.V.I. Tenkanen and J. van de Vis, *Gravitational waves from supercooled phase transitions: dimensional transmutation meets dimensional reduction*, *JHEP* **02** (2024) 234 [arXiv:2312.12413] [INSPIRE].

[26] J. Chakrabortty and S. Mohanty, *One Loop Thermal Effective Action*, arXiv:2411.14146 [INSPIRE].

[27] P.M. Schicho, T.V.I. Tenkanen and J. Österman, *Robust approach to thermal resummation: Standard Model meets a singlet*, *JHEP* **06** (2021) 130 [arXiv:2102.11145] [INSPIRE].

[28] M. Chala, J.C. Criado, L. Gil and J.L. Miras, *Higher-order-operator corrections to phase-transition parameters in dimensional reduction*, *JHEP* **10** (2024) 025 [arXiv:2406.02667] [INSPIRE].

[29] M. Chala and G. Guedes, *The high-temperature limit of the SM(EFT)*, *JHEP* **07** (2025) 085 [arXiv:2503.20016] [INSPIRE].

[30] K. Farakos, K. Kajantie, K. Rummukainen and M.E. Shaposhnikov, *3-d physics and the electroweak phase transition: a framework for lattice Monte Carlo analysis*, *Nucl. Phys. B* **442** (1995) 317 [hep-lat/9412091] [INSPIRE].

[31] M. Laine, *Exact relation of lattice and continuum parameters in three-dimensional SU(2) + Higgs theories*, *Nucl. Phys. B* **451** (1995) 484 [hep-lat/9504001] [INSPIRE].

[32] M. Laine and A. Rajantie, *Lattice continuum relations for 3-D SU(N) + Higgs theories*, *Nucl. Phys. B* **513** (1998) 471 [hep-lat/9705003] [INSPIRE].

JHEP08(2025)109

[33] M. Luscher, *Chiral gauge theories revisited*, *Subnucl. Ser.* **38** (2002) 41 [hep-th/0102028] [INSPIRE].

[34] Y. Aoki, F. Csikor, Z. Fodor and A. Ukawa, *The endpoint of the first order phase transition of the SU(2) gauge Higgs model on a four-dimensional isotropic lattice*, *Phys. Rev. D* **60** (1999) 013001 [hep-lat/9901021] [INSPIRE].

[35] F. Csikor et al., *Electroweak phase transition in the MSSM: 4-Dimensional lattice simulations*, *Phys. Rev. Lett.* **85** (2000) 932 [hep-ph/0001087] [INSPIRE].

[36] M. Hindmarsh, S.J. Huber, K. Rummukainen and D.J. Weir, *Numerical simulations of acoustically generated gravitational waves at a first order phase transition*, *Phys. Rev. D* **92** (2015) 123009 [arXiv:1504.03291] [INSPIRE].

[37] E.J. Weinberg, *Vacuum decay in theories with symmetry breaking by radiative corrections*, *Phys. Rev. D* **47** (1993) 4614 [hep-ph/9211314] [INSPIRE].

[38] D. Metaxas and E.J. Weinberg, *Gauge independence of the bubble nucleation rate in theories with radiative symmetry breaking*, *Phys. Rev. D* **53** (1996) 836 [hep-ph/9507381] [INSPIRE].

[39] M. Garny and T. Konstandin, *On the gauge dependence of vacuum transitions at finite temperature*, *JHEP* **07** (2012) 189 [arXiv:1205.3392] [INSPIRE].

[40] R. Fukuda and T. Kugo, *Gauge Invariance in the Effective Action and Potential*, *Phys. Rev. D* **13** (1976) 3469 [INSPIRE].

[41] S.P. Martin and H.H. Patel, *Two-loop effective potential for generalized gauge fixing*, *Phys. Rev. D* **98** (2018) 076008 [arXiv:1808.07615] [INSPIRE].

[42] D. Croon, V. Sanz and G. White, *Model Discrimination in Gravitational Wave spectra from Dark Phase Transitions*, *JHEP* **08** (2018) 203 [arXiv:1806.02332] [INSPIRE].

[43] C. Han, K.-P. Xie, J.M. Yang and M. Zhang, *Self-interacting dark matter implied by nano-Hertz gravitational waves*, *Phys. Rev. D* **109** (2024) 115025 [arXiv:2306.16966] [INSPIRE].

[44] A. Banik, Y. Cui, Y.-D. Tsai and Y. Tsai, *The Sound of Dark Sectors in Pulsar Timing Arrays*, arXiv:2412.16282 [INSPIRE].

[45] H. Kleinert, *Disorder version of the Abelian Higgs model and the order of the superconductive phase transition*, *Lett. Nuovo Cim.* **35** (1982) 405 [INSPIRE].

[46] C. Dasgupta and B.I. Halperin, *Phase Transition in a Lattice Model of Superconductivity*, *Phys. Rev. Lett.* **47** (1981) 1556 [INSPIRE].

[47] B. Halperin, T.C. Lubensky and S.-K. Ma, *First order phase transitions in superconductors and smectic A liquid crystals*, *Phys. Rev. Lett.* **32** (1974) 292 [INSPIRE].

[48] K. Kajantie et al., *Vortex tension as an order parameter in three-dimensional U(1) + Higgs theory*, *Nucl. Phys. B* **546** (1999) 351 [hep-ph/9809334] [INSPIRE].

[49] K. Kajantie, M. Karjalainen, M. Laine and J. Peisa, *Masses and phase structure in the Ginzburg-Landau model*, *Phys. Rev. B* **57** (1998) 3011 [cond-mat/9704056] [INSPIRE].

[50] S. Mo, J. Hove and A. Sudbo, *The order of the metal to superconductor transition*, *Phys. Rev. B* **65** (2002) 104501 [cond-mat/0109260] [INSPIRE].

[51] I.F. Herbut and Z. Tesanovic, *Critical fluctuations in superconductors and the magnetic field penetration depth*, *Phys. Rev. Lett.* **76** (1996) 4588 [cond-mat/9605185] [INSPIRE].

[52] K. Kajantie et al., *Thermodynamics of gauge invariant U(1) vortices from lattice Monte Carlo simulations*, *Phys. Lett. B* **428** (1998) 334 [hep-ph/9803367] [INSPIRE].

JHEP08(2025)109

[53] K. Kajantie et al., *Statistical mechanics of vortices from field theory*, *Nucl. Phys. B* **559** (1999) 395 [hep-lat/9906028] [INSPIRE].

[54] M.B. Hindmarsh and T.W.B. Kibble, *Cosmic strings*, *Rept. Prog. Phys.* **58** (1995) 477 [hep-ph/9411342] [INSPIRE].

[55] G. Vincent, N.D. Antunes and M. Hindmarsh, *Numerical simulations of string networks in the Abelian Higgs model*, *Phys. Rev. Lett.* **80** (1998) 2277 [hep-ph/9708427] [INSPIRE].

[56] M. Hindmarsh et al., *Scaling from gauge and scalar radiation in Abelian Higgs string networks*, *Phys. Rev. D* **96** (2017) 023525 [arXiv:1703.06696] [INSPIRE].

[57] I. Baldes and M.O. Olea-Romacho, *Primordial black holes as dark matter: interferometric tests of phase transition origin*, *JHEP* **01** (2024) 133 [arXiv:2307.11639] [INSPIRE].

[58] Y. Gouttenoire, *Primordial black holes from conformal Higgs*, *Phys. Lett. B* **855** (2024) 138800 [arXiv:2311.13640] [INSPIRE].

[59] M. Lewicki, P. Toczek and V. Vaskonen, *Black holes and gravitational waves from phase transitions in realistic models*, arXiv:2412.10366 [INSPIRE].

[60] G. Franciolini, Y. Gouttenoire and R. Jinno, *Curvature Perturbations from First-Order Phase Transitions: Implications to Black Holes and Gravitational Waves*, arXiv:2503.01962 [INSPIRE].

[61] M. Kierkla, N. Ramberg, P. Schicho and D. Schmitt, *Theoretical uncertainties for primordial black holes from cosmological phase transitions*, arXiv:2506.15496 [INSPIRE].

[62] O. Gould and J. Hirvonen, *Effective field theory approach to thermal bubble nucleation*, *Phys. Rev. D* **104** (2021) 096015 [arXiv:2108.04377] [INSPIRE].

[63] A. Ekstedt, O. Gould and J. Löfgren, *Radiative first-order phase transitions to next-to-next-to-leading order*, *Phys. Rev. D* **106** (2022) 036012 [*Erratum ibid.* **110** (2024) 019901] [arXiv:2205.07241] [INSPIRE].

[64] O. Gould and T.V.I. Tenkanen, *Perturbative effective field theory expansions for cosmological phase transitions*, *JHEP* **01** (2024) 048 [arXiv:2309.01672] [INSPIRE].

[65] A.D. Linde, *Infrared Problem in Thermodynamics of the Yang-Mills Gas*, *Phys. Lett. B* **96** (1980) 289 [INSPIRE].

[66] P.B. Arnold and O. Espinosa, *The effective potential and first order phase transitions: beyond leading-order*, *Phys. Rev. D* **47** (1993) 3546 [*Erratum ibid.* **50** (1994) 6662] [hep-ph/9212235] [INSPIRE].

[67] J. Löfgren, *Stop comparing resummation methods*, *J. Phys. G* **50** (2023) 125008 [arXiv:2301.05197] [INSPIRE].

[68] T. Matsubara, *A new approach to quantum statistical mechanics*, *Prog. Theor. Phys.* **14** (1955) 351 [INSPIRE].

[69] K. Farakos, K. Kajantie, K. Rummukainen and M.E. Shaposhnikov, *3-D physics and the electroweak phase transition: perturbation theory*, *Nucl. Phys. B* **425** (1994) 67 [hep-ph/9404201] [INSPIRE].

[70] J. Hirvonen et al., *Computing the gauge-invariant bubble nucleation rate in finite temperature effective field theory*, *JHEP* **07** (2022) 135 [arXiv:2112.08912] [INSPIRE].

[71] M. Kierkla et al., *Finite-temperature bubble nucleation with shifting scale hierarchies*, *JHEP* **07** (2025) 153 [arXiv:2503.13597] [INSPIRE].

JHEP08(2025)109

[72] O. Gould and P.M. Saffin, *Perturbative gravitational wave predictions for the real-scalar extended Standard Model*, *JHEP* **03** (2025) 105 [arXiv:2411.08951] [INSPIRE].

[73] A. Ekstedt, P. Schicho and T.V.I. Tenkanen, *DRalgo: a package for effective field theory approach for thermal phase transitions*, *Comput. Phys. Commun.* **288** (2023) 108725 [arXiv:2205.08815] [INSPIRE].

[74] K. Kajantie, K. Rummukainen and M.E. Shaposhnikov, *A Lattice Monte Carlo study of the hot electroweak phase transition*, *Nucl. Phys. B* **407** (1993) 356 [hep-ph/9305345] [INSPIRE].

[75] A. Jakovac, K. Kajantie and A. Patkos, *A hierarchy of effective field theories of hot electroweak matter*, *Phys. Rev. D* **49** (1994) 6810 [hep-ph/9312355] [INSPIRE].

[76] A. Ekstedt, P. Schicho and T.V.I. Tenkanen, *Cosmological phase transitions at three loops: the final verdict on perturbation theory*, *Phys. Rev. D* **110** (2024) 096006 [arXiv:2405.18349] [INSPIRE].

[77] M. Bertenstam et al., *Gravitational waves from color restoration in a leptoquark model of radiative neutrino masses*, arXiv:2501.01286 [INSPIRE].

[78] M. Hindmarsh, S.J. Huber, K. Rummukainen and D.J. Weir, *Shape of the acoustic gravitational wave power spectrum from a first order phase transition*, *Phys. Rev. D* **96** (2017) 103520 [*Erratum ibid.* **101** (2020) 089902] [arXiv:1704.05871] [INSPIRE].

[79] F. Giese, T. Konstandin and J. van de Vis, *Model-independent energy budget of cosmological first-order phase transitions — A sound argument to go beyond the bag model*, *JCAP* **07** (2020) 057 [arXiv:2004.06995] [INSPIRE].

[80] T.V.I. Tenkanen and J. van de Vis, *Speed of sound in cosmological phase transitions and effect on gravitational waves*, *JHEP* **08** (2022) 302 [arXiv:2206.01130] [INSPIRE].

[81] L. Husdal, *On Effective Degrees of Freedom in the Early Universe*, *Galaxies* **4** (2016) 78 [arXiv:1609.04979] [INSPIRE].

[82] T. Bringmann et al., *Hunting WIMPs with LISA: correlating dark matter and gravitational wave signals*, *JCAP* **05** (2024) 065 [arXiv:2311.06346] [INSPIRE].

[83] K. Kajantie, M. Laine, K. Rummukainen and M.E. Shaposhnikov, *The electroweak phase transition: a Nonperturbative analysis*, *Nucl. Phys. B* **466** (1996) 189 [hep-lat/9510020] [INSPIRE].

[84] J.L. Cardy, *Scaling and renormalization in statistical physics*, Cambridge University Press (1996) [INSPIRE].

[85] M. Laine, M. Meyer and G. Nardini, *Thermal phase transition with full 2-loop effective potential*, *Nucl. Phys. B* **920** (2017) 565 [arXiv:1702.07479] [INSPIRE].

[86] D. Curtin, J. Roy and G. White, *Gravitational waves and tadpole resummation: efficient and easy convergence of finite temperature QFT*, *Phys. Rev. D* **109** (2024) 116001 [arXiv:2211.08218] [INSPIRE].

[87] M. Laine and M. Losada, *Two loop dimensional reduction and effective potential without temperature expansions*, *Nucl. Phys. B* **582** (2000) 277 [hep-ph/0003111] [INSPIRE].

[88] V. Guada, M. Nemevšek and M. Pintar, *FindBounce: package for multi-field bounce actions*, *Comput. Phys. Commun.* **256** (2020) 107480 [arXiv:2002.00881] [INSPIRE].

[89] J. Löfgren, M.J. Ramsey-Musolf, P. Schicho and T.V.I. Tenkanen, *Nucleation at Finite Temperature: a Gauge-Invariant Perturbative Framework*, *Phys. Rev. Lett.* **130** (2023) 251801 [arXiv:2112.05472] [INSPIRE].

JHEP08(2025)109

[90] O. Gould and T.V.I. Tenkanen, *On the perturbative expansion at high temperature and implications for cosmological phase transitions*, *JHEP* **06** (2021) 069 [arXiv:2104.04399] [INSPIRE].

[91] C. Grojean and G. Servant, *Gravitational Waves from Phase Transitions at the Electroweak Scale and Beyond*, *Phys. Rev. D* **75** (2007) 043507 [hep-ph/0607107] [INSPIRE].

[92] C. Delaunay, C. Grojean and J.D. Wells, *Dynamics of Non-renormalizable Electroweak Symmetry Breaking*, *JHEP* **04** (2008) 029 [arXiv:0711.2511] [INSPIRE].

[93] G.C. Dorsch, S.J. Huber, T. Konstandin and J.M. No, *A Second Higgs Doublet in the Early Universe: Baryogenesis and Gravitational Waves*, *JCAP* **05** (2017) 052 [arXiv:1611.05874] [INSPIRE].

[94] J. Ellis, M. Lewicki and J.M. No, *On the Maximal Strength of a First-Order Electroweak Phase Transition and its Gravitational Wave Signal*, *JCAP* **04** (2019) 003 [arXiv:1809.08242] [INSPIRE].

[95] A. Ekstedt, *Higher-order corrections to the bubble-nucleation rate at finite temperature*, *Eur. Phys. J. C* **82** (2022) 173 [arXiv:2104.11804] [INSPIRE].

[96] A. Ekstedt, O. Gould and J. Hirvonen, *BubbleDet: a Python package to compute functional determinants for bubble nucleation*, *JHEP* **12** (2023) 056 [arXiv:2308.15652] [INSPIRE].

[97] A. Ekstedt, *Convergence of the nucleation rate for first-order phase transitions*, *Phys. Rev. D* **106** (2022) 095026 [arXiv:2205.05145] [INSPIRE].

[98] P. Athron, L. Morris and Z. Xu, *How robust are gravitational wave predictions from cosmological phase transitions?*, *JCAP* **05** (2024) 075 [arXiv:2309.05474] [INSPIRE].

[99] K. Enqvist, J. Ignatius, K. Kajantie and K. Rummukainen, *Nucleation and bubble growth in a first order cosmological electroweak phase transition*, *Phys. Rev. D* **45** (1992) 3415 [INSPIRE].

[100] J.M. Cornwall, R. Jackiw and E. Tomboulis, *Effective Action for Composite Operators*, *Phys. Rev. D* **10** (1974) 2428 [INSPIRE].

[101] J. Berges, *Introduction to nonequilibrium quantum field theory*, *AIP Conf. Proc.* **739** (2004) 3 [hep-ph/0409233] [INSPIRE].

[102] K. Kainulainen and O. Koskivaara, *Non-equilibrium dynamics of a scalar field with quantum backreaction*, *JHEP* **12** (2021) 190 [arXiv:2105.09598] [INSPIRE].

[103] M. Hindmarsh, S.J. Huber, K. Rummukainen and D.J. Weir, *Gravitational waves from the sound of a first order phase transition*, *Phys. Rev. Lett.* **112** (2014) 041301 [arXiv:1304.2433] [INSPIRE].

[104] G.D. Moore and K. Rummukainen, *Electroweak bubble nucleation, nonperturbatively*, *Phys. Rev. D* **63** (2001) 045002 [hep-ph/0009132] [INSPIRE].

[105] M.A. Ajmi and M. Hindmarsh, *Thermal suppression of bubble nucleation at first-order phase transitions in the early Universe*, *Phys. Rev. D* **106** (2022) 023505 [arXiv:2205.04097] [INSPIRE].

[106] H.-K. Guo et al., *Estimating the uncertainty of cosmological first order phase transitions with numerical simulations of bubble nucleation*, *Phys. Rev. D* **110** (2024) 063541 [arXiv:2310.04654] [INSPIRE].

[107] O. Gould, A. Kormu and D.J. Weir, *Nonperturbative test of nucleation calculations for strong phase transitions*, *Phys. Rev. D* **111** (2025) L051901 [arXiv:2404.01876] [INSPIRE].

JHEP08(2025)109

[108] A.H. Guth and S.H.H. Tye, *Phase Transitions and Magnetic Monopole Production in the Very Early Universe*, *Phys. Rev. Lett.* **44** (1980) 631 [*Erratum ibid.* **44** (1980) 963] [INSPIRE].

[109] A.H. Guth and E.J. Weinberg, *Cosmological Consequences of a First Order Phase Transition in the SU(5) Grand Unified Model*, *Phys. Rev. D* **23** (1981) 876 [INSPIRE].

[110] M.S. Turner, E.J. Weinberg and L.M. Widrow, *Bubble nucleation in first order inflation and other cosmological phase transitions*, *Phys. Rev. D* **46** (1992) 2384 [INSPIRE].

[111] O. Gould, S. Güyer and K. Rummukainen, *First-order electroweak phase transitions: a nonperturbative update*, *Phys. Rev. D* **106** (2022) 114507 [*Erratum ibid.* **110** (2024) 119903] [arXiv:2205.07238] [INSPIRE].

[112] C. Caprini et al., *Detecting gravitational waves from cosmological phase transitions with LISA: an update*, *JCAP* **03** (2020) 024 [arXiv:1910.13125] [INSPIRE].

[113] S. Kawamura et al., *The japanese space gravitational wave antenna: DECIGO*, *Class. Quant. Grav.* **28** (2011) 094011 [INSPIRE].

[114] LISA collaboration, *Laser Interferometer Space Antenna*, arXiv:1702.00786 [INSPIRE].

[115] L.S. Friedrich, M.J. Ramsey-Musolf, T.V.I. Tenkanen and V.Q. Tran, *Addressing the Gravitational Wave - Collider Inverse Problem*, arXiv:2203.05889 [INSPIRE].

[116] J. Fuentes-Martín et al., *A proof of concept for matchete: an automated tool for matching effective theories*, *Eur. Phys. J. C* **83** (2023) 662 [arXiv:2212.04510] [INSPIRE].

[117] R.M. Fonseca, *GroupMath: a Mathematica package for group theory calculations*, *Comput. Phys. Commun.* **267** (2021) 108085 [arXiv:2011.01764] [INSPIRE].

[118] K. Kajantie et al., *Nonperturbative Debye mass in finite temperature QCD*, *Phys. Rev. Lett.* **79** (1997) 3130 [hep-ph/9708207] [INSPIRE].

[119] K. Kajantie, M. Laine, K. Rummukainen and Y. Schroder, *How to resum long distance contributions to the QCD pressure?*, *Phys. Rev. Lett.* **86** (2001) 10 [hep-ph/0007109] [INSPIRE].

[120] A. Hart, M. Laine and O. Philipsen, *Static correlation lengths in QCD at high temperatures and finite densities*, *Nucl. Phys. B* **586** (2000) 443 [hep-ph/0004060] [INSPIRE].

[121] M. Lewicki et al., *Impact of theoretical uncertainties on model parameter reconstruction from GW signals sourced by cosmological phase transitions*, *Phys. Rev. D* **110** (2024) 023538 [arXiv:2403.03769] [INSPIRE].

[122] B. Bunk, E.-M. Ilgenfritz, J. Kripfganz and A. Schiller, *The finite temperature phase transition in lattice SU(2) Higgs theory at weak couplings*, *Nucl. Phys. B* **403** (1993) 453 [INSPIRE].

[123] Z. Fodor et al., *Simulating the electroweak phase transition in the SU(2) Higgs model*, *Nucl. Phys. B* **439** (1995) 147 [hep-lat/9409017] [INSPIRE].

[124] F. Csikor, Z. Fodor, J. Hein and J. Heitger, *Interface tension of the electroweak phase transition*, *Phys. Lett. B* **357** (1995) 156 [hep-lat/9506029] [INSPIRE].

[125] L. Niemi, M.J. Ramsey-Musolf, T.V.I. Tenkanen and D.J. Weir, *Thermodynamics of a Two-Step Electroweak Phase Transition*, *Phys. Rev. Lett.* **126** (2021) 171802 [arXiv:2005.11332] [INSPIRE].

[126] D.E. Morrissey and M.J. Ramsey-Musolf, *Electroweak baryogenesis*, *New J. Phys.* **14** (2012) 125003 [arXiv:1206.2942] [INSPIRE].

[127] C. Caprini et al., *Science with the space-based interferometer eLISA. II: Gravitational waves from cosmological phase transitions*, *JCAP* **04** (2016) 001 [arXiv:1512.06239] [INSPIRE].

JHEP08(2025)109

[128] C. Arzt, *Reduced effective Lagrangians*, *Phys. Lett. B* **342** (1995) 189 [hep-ph/9304230] [INSPIRE].

[129] H. Georgi, *On-shell effective field theory*, *Nucl. Phys. B* **361** (1991) 339 [INSPIRE].

[130] J. Aebischer, A.J. Buras and J. Kumar, *Simple rules for evanescent operators in one-loop basis transformations*, *Phys. Rev. D* **107** (2023) 075007 [arXiv:2202.01225] [INSPIRE].

[131] J.C. Collins and J.A.M. Vermaseren, *Axodraw Version 2*, arXiv:1606.01177 [INSPIRE].

[132] I. Ghisoiu, J. Moller and Y. Schroder, *Debye screening mass of hot Yang-Mills theory to three-loop order*, *JHEP* **11** (2015) 121 [arXiv:1509.08727] [INSPIRE].

[133] F. Bernardo, P. Klose, P. Schicho and T.V.I. Tenkanen, *Higher-dimensional operators at finite-temperature affect gravitational-wave predictions* [Data set], Zenodo (2025), DOI:10.5281/zenodo.16753884.

JHEP08(2025)109